African Journal of
Biochemistry and Molecular Biology Research

ISSN : 1595-7926

Index: Harvard, Boston, Sydney University, Dimensions, Lens, ResearchGet Scilit, Semantic, Google Scholar, Base etc

https://doi.org/10.58578/AJBMBR.v2i3.8014

Effects of Ferrous Nanoparticles of *Psidium guajava* (Linn.) Leaf on Liver Functions in Male Wistar Rats

Musa Azegya Mustapha, Arowora K. A, Ezeonu C. S, Isaac John Umaru
Federal University Wukari, Taraba, Nigeria
maryathanasius@gmail.com

Article Info:

Submitted:	Revised:	Accepted:	Published:
Oct 14, 2025	Nov 5, 2025	Nov 17, 2025	Nov 22, 2025

Abstract

This study evaluated the effects of ferrous nanoparticles (FeNPs) derived from *Psidium guajava* L. leaves on liver function in male Wistar rats. Fresh leaves were harvested from the Government Reservation Area (G.R.A), Wukari, Taraba State, washed, air-dried, and pulverized prior to FeNP preparation. Twenty-five male albino rats (140–190 g) were randomly assigned to five groups, with Group 1 serving as the control and Groups 2–5 receiving oral FeNP doses of 100, 250, 500, and 1000 ppm, respectively, for three weeks. Post-treatment, serum samples were collected under chloroform anaesthesia for biochemical and histological analyses. Liver function tests revealed non-significant differences ($p > 0.05$) in measured parameters between Groups 1 and 3, whereas Groups 2, 4, and 5 showed significant alterations ($p < 0.05$) compared with the control. Aspartate aminotransferase (AST) levels increased significantly in Groups 3–5, while Group 2 showed no significant change; alanine aminotransferase (ALT) levels increased significantly in all treated groups except Groups 3 and 4. Albumin concentrations were significantly elevated across all treated groups. Total bilirubin (TB) and indirect bilirubin (IDB) remained unchanged in Group 2 but increased significantly in Groups 3–5, whereas direct bilirubin (DB) did

not differ in Groups 2 and 3 but rose significantly in Groups 4 and 5. Total protein (TP) levels were comparable between Groups 1 and 2 but were significantly higher in Groups 3–5. Malondialdehyde (MDA) levels did not differ significantly among groups, although apparent increases were observed, while catalase (CAT) activity was significantly elevated in all treated groups, peaking in Group 5. Superoxide dismutase (SOD) activity remained unchanged in Groups 2 and 3 but increased significantly in Groups 4 and 5. Histological examination revealed dose-dependent structural abnormalities in liver tissue, with the most pronounced damage observed in Group 5. Overall, FeNPs from *Psidium guajava* leaves induced dose-dependent alterations in liver function and antioxidant enzyme activity in male Wistar rats, with higher doses, particularly 1000 ppm, associated with marked biochemical disturbances and histological damage, suggesting potential hepatotoxicity at elevated concentrations and underscoring the need for further studies to define safe exposure thresholds and long-term effects.

Keywords: Ferrous Nanoparticles; *Psidium guajava*; Liver Function; Antioxidant Enzymes; Male Wistar Rats; Hepatotoxicity

INTRODUCTION

Nanotechnology is the science of structuring matters into a large surface area which holistically possesses unique characteristics. National Nanotechnology initiative established a generalized description that it was about manipulation of matter with at least one-dimensional size from 1 – 100nm (Barbara and Nora, 2005). Nanotechnology may be able to create many new materials and devices with a vast range of applications, such as in medicine, electronics, biomaterials, and energy production (Saini, 2013). Nanotechnology deals with matter at the scale of one billionth of meter (10−9 m). According to the classic definition, nanomaterials are those materials whose key physical characteristics are dictated by the nano-objects they contain (Iqbal et al., 2017).

An expanding field of study is the green production of nanoparticles, which is a well-known substitute for conventional techniques (Arowora et al., 2023). This method utilizes plant extracts for the biosynthesis of nanoparticles. The advantages of green syntheses over chemical and physical approaches include environmental friendliness, cost effectiveness, and ease of scaling up for large-scale nanoparticle production. In addition, there is no need to utilize harmful compounds or high temperatures, pressures, or energy (David et al., 2014; Arowora et al., 2023).

Plants are predominant natural source of numerous bioactive compounds (Newman et al., 2003; Kumar et al., 2021). Several diseases have been cured using a variety of plant preparations in folk medicine since ancient times (Kumar et al., 2021) and presently, cosmetic, pharmaceutical, and nutraceutical industries are paying more attention to plant preparations and pure phytochemicals. Medicinal plants contain natural products that are important in pharmaceutical development and used to remedy a variety of ailments in humans (Salau et al., 2013; Imo and Zaku, 2019; Yakubu et al., 2020). Some of the medicinal plants have been investigated in the laboratory for their medicinal uses (Imo and Uhegbu, 2015).

The liver, being one of the most crucial organs, is the main target for any routes of exposure involving bloodstream translocation, and prior studies have demonstrated a significant accumulation of nanoparticles (NPs) inside the liver following injection (Hirn et al., 2011), retention of particles in the liver after ingestion (Schleh et al., 2012; Arowora et al., 2023), and affected liver after inhalation.

The liver is one of the most essential organ in the body since it is in charge of regulating critical biochemical and other functional activities such as maintaining homeostasis, supplying energy and nutrients, and detoxifying foreign substances such as medications and other toxicants (Eesha et al., 2011; Arfat et al., 2014; Sowemimo et al., 2015; Imo et al., 2021). The liver is responsible for xenobiotic biotransformation. Native (endogenous) chemicals released by physiological processes, such as fatty acids, bilirubin, thyroxin, other steroid hormones are metabolized by the hepatocytes (Modusolumuo, 2011).

The guava (Psidium guajava L.) tree belonging to the Myrtaceae family, is a very unique and traditional plant which is grown due to its diverse medicinal and nutritive properties (Kumar et al., 2021). Guava leaves are the rich source of minerals, such as calcium, potassium, sulfur, sodium, iron, boron, magnesium, manganese, and vitamins C and B. The higher concentrations of Mg, Na, S, Mn, and B in guava leaves makes them a highly suitable choice for human nutrition and also as an animal feed to prevent micronutrient deficiency (Kumar et al., 2021). Thomas et al. (2017) reported the concentration of minerals such as Ca, P, K, Fe, and Mg as 1660, 360, 1602, 13.50, and 440 mg per 100g of guava leaf dry weight (DW), respectively. The concentration of vitamins C and B was 103.0 and 14.80 mg per 100g DW, respectively. Guava leaves also contains

9.73% protein on a dry weight basis (Rahman et al., 2013). Proteins are large biomolecules composed of amino acids and act as building blocks of cells. Proteins play a major role in growth and maintenance, enzyme regulation, and cell signaling, and also as biocatalysts (Albert et al., 2002). Recently, plant-based nutrients have gained potential because of the high demand for nutritionally rich food, particularly protein. A great effort is now being made to find highly sustainable nutritionally rich food sources (Lonnie et al., 2018). Thomas et al. (2017) reported 16.8 mg protein/100g and 8 mg amino acids/100g in guava leaves as estimated according to Lowry's and ninhydrin methods, respectively. Jassal et al. (2019) reported that guava leaves can be utilized as a novel and sustainable dietary source as they are a rich source of proteins, carbohydrates, and dietary fibers. Different parts of the guava tree, i.e., roots, leaves, bark, stem, and fruits, have been employed for treating stomach ache, diabetes, diarrhea, and other health ailments in many countries (Kumar et al., 2021). Guava leaves (Psidium guajavae folium) are dark green, elliptical, oval, and characterized by their obtuse-type apex. Guava leaves, along with the pulp and seeds, are used to treat certain respiratory and gastrointestinal disorders, and to increase platelets in patients suffering from dengue fever (Laily et al., 2015). Guava leaves (GLs) are also widely used for their antispasmodic, cough sedative, anti-inflammatory, antidiarrheic, antihypertension, antiobesity, and antidiabetic properties (Chen et al., 2007).

The objectives of this study were to: Produce green-synthesized ferrous nanoparticles from aqueous leaf extracts of guava leaf , Determine the levels of selected liver function indices: aspartate aminotransferase (AST), alanine aminotransferase (ALT), alkaline phosphatase (ALP), total protein (TP) and albumin (ALB) direct bilirubin (DB), total bilirubin (TB) and indirect bilirubin (IDB) in rats administered ferrous nanoparticles from extracts of Psidium guajava, Determine the effects of guava leaf ferrous nanoparticles on antioxidant enzymes superoxide dismutase (SOD), catalase (CAT), and lipid peroxidation parameter Malondialdehyde (MDA) and examine the effect of FeNPs on histopathology of liver in male wistar rats

Scope of the Study; This study focused solely on chemical composition (vitamins, minerals and phytochemicals) of Psidium gujava leaf and assessed the biological impact of its ferrous nanoparticles on liver functions in male Wistar rats.

Figure 1: *Psidium guajava* plant in its habitat, with few fruits and flowers (Patil and Rane, 2020).

MATERIALS AND METHODS

Materials

Glassware and Facilities

Mortar and pestle, digital analytical weighing balance (ohaus: pa-1000), beakers, whatman number 1 filter paper, conical flask, spatula, measuring cylinder, aluminum foil, cotton wool, sample bottles, separating funnel, plastic funnels, thermostatic water cabinet (Model:HH-W420), Spectrophotometer(UV-Visible double beam light), micro pipette, liston classic centrifuge (C2204), sykam HPLC (S3250 UV/visible detector). Micropipettes, Cuvettes and test tube.

Reagents and Chemicals

Ferric chloride (FeCl3), ethanol, water, sodium carbonate, trichloroacetic acid (TCA), normal saline. The rest of the chemicals were of analytical grade, Reagents used for the assays were products of Bioscience commercial kits and Spectrum commercial assay kits.

3.1.3 Collection and Preparation of Plant Materials

The fresh leaf of Psidium guajava were collected from Government reservation Area (G.R.A) Wukari, Taraba State. The guava leaf collected were washed several times with water and rinsed with distilled water for the removal of impurities. The washed leaf obtained were air dried until they become crispy, after which they were pulverized in a clean and dry mortar and pestle.

3.1.4 Animal Care and Management

Twenty-five (25) male wistar rats were purchased from Enugu, Enugu State and weighed accordingly and their respective weight noted. They were kept in cages covered with net in a standard environment and acclimatized for one week prior the commencement of the experiment. The rats were fed ad- libitum with commercial feed and water; their bedding was changed every 72hrs to maintain cleanliness and prevent accumulation of ammonia gas.

Methods

Vitamins Profile of Guava Leaf Sample

The following vitamin levels (vitamins K, B1, B9, A and E) were determined using high performance liquid chromatography (HPLC).

Principle: Stationary Phase: A column packed with small, porous particles (stationary phase) retains the sample components based on their interactions with the stationary phase.

Mobile Phase: A liquid solvent (mobile phase) is forced through the column under high pressure, carrying the sample components.

Separation: Components of the sample interact differently with the stationary phase, causing them to move through the column at different rates and separate from each other.

Detection: As the separated components exit the column, they are detected and quantified by a suitable detector, producing a chromatogram (Aryal, 2024).

Methodology: The extract was diluted with the same solvent used for extraction.

Two (2ml) of guava leaf ethanol extract was diluted and filtered with 0.45um syringe filter into the vial. The mobile phase is composed of the following solvents (water, methanol, ethanol and buffer).

The vials were labelled appropriately and placed in the auto sampler of the HPLC for analysis.

The wavelength was set at 230nm to run for 10 minutes using the Reprosil 100, C8, 5um, 4,6 x 150mm column. The sequence was run and observed the retention time and peaks in the chromatogram and then the chromatogram was printed.

Determination of Minerals Composition

Atomic Absorption Spectroscopy (AA S) was used for the determination of minerals in guava leaf sample.

Principle

The principle of AAS is based on the fact that atoms or ions of a specific element can absorb light at unique, characteristic wavelengths. When a sample containing a particular element is exposed to light at that element's specific wavelength, the atoms or ions of that element absorb the light, causing electrons to transition from a ground state to excited states. The amount of light absorbed is directly proportional to the concentration of the absorbing atoms or ions in the sample.

Procedure

Atomization: The sample is atomized, typically using heated graphite tube (Electrothermal AAS) to convert the metal compounds in the sample into free gaseous atoms.

Light Source: Light from a radiation source, usually a hollow-cathode lamp specific to the element being analyzed. This was passed through the cloud of free atoms. This lamp emits light at the precise wavelength that the target element's atoms absorb.

Absorption: The free atoms of the target element in the sample absorbs some of the light from the lamp.

Monochromator: A monochromator is used to isolate the specific wavelength of light absorbed by the analyte from other wavelengths.

Detection: A detector measures the intensity of the light beam after it has passed through the atomized sample. The decrease in light intensity is measured as absorbance.

Concentration determination: The measured absorbance is directly related to the concentration of the element in the sample, following Beer's law. The concentration is

typically determined by comparing the sample's absorbance to a calibration curve generated using solutions of known concentrations of the element.

Preparation of Guava Leaf Extract

The extract was prepared with slight modification on the method reported by (Saranyaadevi et al., 2014). Exactly, 50g of the Psidium guajava leaf were weighed and transferred into 250mL beaker containing 500mL distilled water and was heated at 60ºC, stirred for 30mins, after that, it was covered with cotton wool and aluminum foil and allowed to stay for 24 hours.

3.2.5 Formation of FeNPs

After 24 hours, the leaf was collected and filtered using Whatman No. 1 filter paper. 0.1622g of 1mM Ferric chloride (FeCl3) was weighed and added into 1000 ml of distilled water, 1000 ml aqueous solution of Ferric chloride was prepared into 1000 ml flask, and 150 ml of the Psidium guajava filtrate was gently added and stir meanwhile the flask was covered with cotton wool and foil paper to avoid exposure to light for 3hours in the water bath for reduction into Fe3+ ions, it was then stored at 4ºC for future used (Saranyaadevi, 2014)

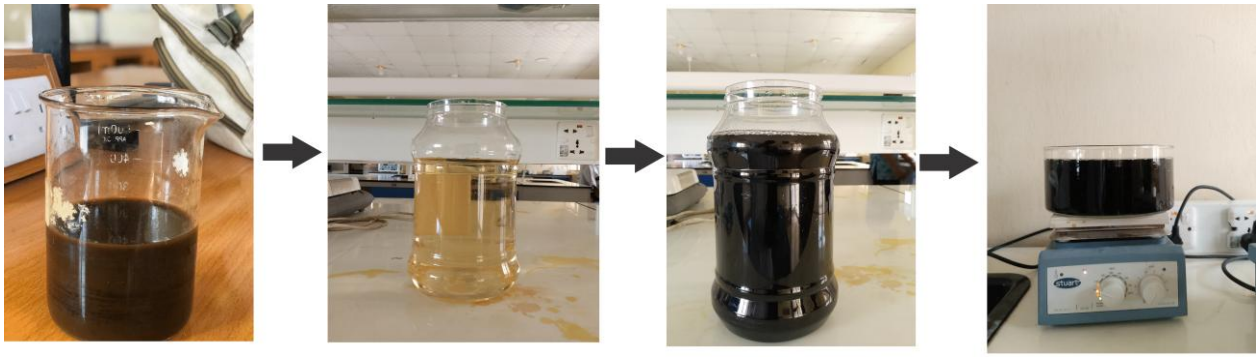

Figure 3.2: Synthesis of ferrous nanoparticles

3.2.6 Characterization of Ferrous Nanoparticles Using UV- Visible Spectroscopy

UV-Visible spectra of synthesized FeNPs were recorded at different time intervals with spectrophotometer with slit width and spectral bandwidth of 1.0 nm. The periodic scans of the optical absorbance between 200 and 500nm with a UV- Vis Spectrophotometer at an interval of 20nm were performed to characterize the ferrous

nanoparticle synthesized from Psidium guajava extract. The bio-reduction process of iron ions in aqueous solution was measured by sampling of 1 ml aliquot compared with 1 ml of distilled water used as blank and subsequently measuring UV-visible spectrum of the solution. UV-visible spectrum was monitored on Shimadzu dual beam spectrophotometer (Model, UV-2500PC Series) operated at a width slit of 20nm within the wavelength range of 200 to 500nm.

Experimental Animals

Male wistar rats weighing between 140 and 190g were used in this experiment. The animals were housed in cages with saw dust as bedding in animal house facility of Department of Biochemistry, Federal University Wukari. All experiments on laboratory rats were performed according to the protocols authorized by Animal Ethical Committee of Department of Biochemistry, Federal University Wukari. The animals were maintained under exposure to a 12h/12h light/dark cycle at room temperature of 25 ± 3oC and free access to standard rats feed and water.

Experimental Design

Twenty-five (25) male wistar rats were purchased from Enugu, Enugu state. They were kept in the animal house of the Department of Biochemistry and acclimatized for two weeks prior to the commencement of the experiment. The rats were administered orally with ferrous nanoparticles based on their body weight. At the end of acclimatization, twenty-five male wistar rats were randomly allotted into five groups of five animals per group and then fed them for three weeks ad-libitum with commercial rat feed and potable water. At the end of the three weeks feeding experiment, the animals were starved overnight and then sacrificed under chloroform anaesthesia.

Experimental Design

Groups	Treatments
1	Rat feed + Potable water (Normal Control)
2	Rat feed + FeNPs 100ppm body weight
3	Rat feed + FeNPs 250ppm body weight
4	Rat feed + FeNPs 500ppm body weight
5	Rat feed + FeNPs 1000ppm body weight

Blood and Tissue Sample Collection

After 21 days, the rats observed an overnight fast and were weighed before sacrificed under chloroform vapor anesthesia. Blood samples were obtained by cardiac puncture using 5ml syringe and 23G needle. Obtained blood samples was then centrifuged at 4000 rpm for 10 minutes to obtain serum for biochemical analysis. Rat livers were harvested and stored in a container of 10% formalin for fixation and then histological photomicrography (Egwaoje et al., 2017).

Tissue Homogenization

The liver of Wistar rats in each group were harvested with utmost care and placed in normal saline (to clean it from any tissue remnants). After weighing, the liver tissues were homogenized in phosphate buffer (1:10 w/v) at 7.4 pH. The supernatants were used for the determination of Thiobarbituric Acid Reactive Substances (TBARS), Superoxide Dismutase (SOD) and Catalase (CAT) (Lowry et al., 1951).

Determination of in-vivo Antioxidant Status in Wistar Rats

Determination of Superoxide Dismutase (SOD) Activity

The assay system for superoxide dismutase was adopted from the method of Nishikimi et al. (1972).

Principle: This assay method is based on measuring superoxide radical production using NADH as an electron donor and PMS as a carrier to reduce NBT to a blue formazan, (NBT) reduction is used as an indicator of $O2^{\bullet-}$ production. SOD will compete with NBT for $O2^{\bullet-}$ Glacial acetic acid lowers the pH of the reaction mixture, thereby stopping the reaction nitroblue tetrazolium. The percent inhibition of NBT reduction is a measure of the amount of SOD.

Procedure: Assay mixture contained 1.2 ml sodium pyrophosphate buffer (pH 7.0, 0.052 mL), 0.1 m1 (186 μL) phenazine methosulphate. 0.3 ml (300 μM) nitroblue tetrazolium. 0.3 mL of the supernatant after centrifugation (1,500 x g for 10 min followed by 10,000 x g for 15 min) of homogenate was added to the reaction mixture. Enzyme reaction was initiated by adding 0.2 mL of NADH (780 uM) and stopped after 1 min by adding 1 mL of glacial acetic acid. Colour intensity of the chromogen was measured at 560 nm

SOD activity in the sample was calculated as follows.

% SOD inhibition=(1-A_S/A_R) ×100

SOD activity (U/ml) =(1-A_S/A_R)×100 ×1.25

Determination of Thiobarbituric Acid Reactive Substance (TBARS)

The Thiobarbituric Acid Reactive substances (TBARS) assay has been widely used as a generic metric of lipid peroxidation in biological fluids. It is often considered a good indicator of the levels of oxidative stress within a biological sample, provided that the sample has been properly handled and stored (Jesús and Chad, 2020).

Principle: The assay involves the reaction of lipid peroxidation products, primarily malondialdehyde (MDA), with thiobarbituric acid (TBA), which leads to the formation of MDA-TBA2 adducts called TBARS. TBARS yields a red-pink color that can be measured spectrophotometrically at 532 nm (Jesús and Chad, 2020).

Procedure: One milliliter of 14% trichloroacetic acid was measured into a test tube, 1mL thiobarbituric acid (0.67%) was then added and 50µL of the tissue homogenate was added.

The mixture was then incubated at 800C for 30 minutes in a water bath. It was allowed to cool rapidly in ice for 5 minutes followed by centrifugation at 3000 x g for 10 minutes.

Malondialdehyde (MDA) was measured spectrophotometrically at 535 nm and the level of lipid peroxidation was calculated using the molar extinction coefficient of malondialdehyde.

Calculation:

Molar extinction of MDA = 1.56 x 105 M-1cm-1

MDA concentration = Absorbance/1.56 x 105 M-1cm-1

Determination of Catalase (CAT) Activity

Catalase activity was determined using the method described by Aebi (1984).

Principle: Catalase detoxifies hydrogen peroxide (H2O2) and converts it to water and molecular oxygen.

$$2\,H_2O_2 \longrightarrow 2H_2O + O_2$$

(Absorbance at 240 nm) (no absorbance at 240 nm)

The catalase activity in the sample was determined by observing the rate of decrease in absorbance at 240 nm.

Procedure: Working buffer (50mM potassium phosphate buffer, pH 7.0, 1000µL) was added to a cuvette and used to standardize the spectrophotometer at a wavelength of 240 nm.

Also, 950 µL of the mixture of working buffer (490µL of 50mM potassium phosphate buffer, pH 7.0) and 460µL of 30 mM hydrogen peroxide (H2O2) was measured at 240 nm every 1 minute for 5 minutes.

Catalase activity was determined and expressed as (U/mL) of the decomposition rate given as (ΔA240 nm/min) of the sample.

ΔA240 nm/min = Change in absorbance per minute

Catalase (U/mL) = (ΔA240 nm/min)/Volume of reaction mixture

Determination of Levels of Serum liver Function Parameters in Rats Administered Ferrous Nanoparticles

Liver Biomarkers were investigated using RANDOX reagent kits and spectrophotometer (VWR UV-6300PC). The blood samples were analysed for aspartate aminotransferase (AST), alanine aminotransferase (ALT), alkaline phosphatase (ALP), Total Protein (TP), Albumin (ALB), direct bilirubin (DB), indirect bilirubin (IND), and Total bilirubin (TB).

Determination of aspartate aminotransferase (AST) activity

A Randox Commercial Enzyme assay kit was used for determination of AST according to the methods of Reitman and Frankel (1957).

Principle: Aspartate aminotransferase (AST) catalyzes the transamination of aspartate to alpha-keto glutarate to form glutamate and oxaloacetate, which then reacts with 2,4-dinitrophenylhydrazine to form hydrazone derivative of oxaloacetate, a coloured complex which can be measured at 546 nm.

Procedure: AST reagent was pipette into a cuvette, it was then incubated at 37°C for a few minutes.

A serum sample was added and mixed. The absorbance was read at 340 nm for 1–3 minutes.

The enzyme activity was calculated using the absorbance change (ΔA/min).

L– aspartate + α – oxoglutarate $\xrightarrow{AST}$ L- glutamate + oxaloacetate.

3.7.2 Determination of alanine aminotransferase (ALT) activity

Alanine aminotransferase was determined as described by Reitman and Frankel, (1957) using assay kits (RANDOX Laboratories Ltd, UK).

Principle: Alanine aminotransferase (ALT) catalyzes the transamination of alanine to alpha-keto glutarate to form glutamate and pyruvic acid, which then reacts with 2,4-dinitrophenylhydrazine to form hydrazone derivative of pyruvate, a coloured complex which can be measured at 546 nm.

α – oxoglutarate + L–alanine ALT L- glutamate + pyruvate

Procedure:

ALT reagent was pipetted into cuvette and pre-warm at 37°C.

Serum of the wister rat was added, and the absorbance was read at 340 nm.

ΔA/min was used to calculate the activity.

Assay for alkaline phosphatase (ALP) activity

This was done using a Commercial Enzyme Kit (AGAPPE) according to the method of Tietz, (1995). The change in absorbance per minute (Δ OD/min) during 3 minutes interval was measured at 405 nm.

Principle: Para-nitrophenylphosphate + H2O ALP p-nitrophenol + Inorganic phosphate

Procedure:

ALP reagent was pipetted into a cuvette, it was then incubated at 37°C for a few minutes.

A serum sample was added and mixed. The absorbance was read at 405 nm at 1minute intervals for 2-3 minutes

The enzyme activity was calculated

Calculation

Equation 1: ALP Activity (U/L) = (Δ OD/min.) x 2750.

Determination of Total Protein

Determinations of total protein was done spectrophotometrically using Randox analytical kits according to standard procedures of manufacturer's protocols (Tietz, 1995).

Principle: Cupric ions in alkaline medium, interact with protein peptide bonds resulting in the formation of a colored complex. The intensity of the color, measured at 546 nm, is directly proportional to the albumin concentration in the sample.

Procedure:

Absorbance was measured at 540–560 nm.

Standard curve was used to calculate total protein.

Biuret reagent was pipette into a cuvette; it was then incubated at room temperature for 10 minutes.

A serum sample was added and mixed. The absorbance was read at 540 – 560 nm.

Standard curve was used to calculate total protein.

Determination of Serum Albumin

Determination of albumin was done spectrophotometrically using Randox analytical kits according to standard procedures of manufacturer's protocols (Tietz, 1995).

Principle: Simple, direct procedure for measuring albumin concentration in biological samples. The improved method utilizes bromocresol green that forms a blue green coloured complex specifically with albumin. The intensity of the colour measured at 630 nm, is directly proportional to the albumin concentration in the sample. The optimized formulation substantially reduces interference by substances in the raw samples.

Procedure:

BCG reagent was added to cuvette and then serum was added, it was then mixed and wait for 30 seconds to 1 minute. The absorbance was read at 620 nm.

Determination of Direct Bilirubin

Principle: Conjugated (direct) bilirubin reacts with diazotized sulfanilic acid to form azobilirubin.

Procedure:

Diazo reagent was added to the test tube, follow by serum

It was incubated for 5 minutes at room temp.

It was measured directly at 540 nm. The calibration curve was read.

Determination of Total Bilirubin

Principle: Both conjugated and unconjugated bilirubin react with diazotized reagents in the presence of an accelerator.

Procedure:

Total bilirubin reagent was added to the cuvette, followed by serum.

It was incubated for 10 minutes. The absorbance was measured at 540 nm.

3.7.8 Determination of Indirect Bilirubin

Indirect Bilirubin = Total Bilirubin -Direct Bilirubin.

Histopathology of Rats livers

This was done according to the methods of (Avwioro, 2011) and (Choji et al., 2015). Tissues were harvested and fixed in 10% formalin for 3 days, cut into thin slices of 5mmX 2mm X 1mm thick and then processed. Tissues were embedded in molten paraffin wax using embedding moulds. The tissues were embedded using embedding cassettes on a tissue Tek Embedding Centre and cooled rapidly on the cooling component. Tissues were sectioned using a rotary microtome set at 4microns, picked on slides and ready for staining. Sections were dewaxed and hydrated by passing through two changes of xylene and through descending grades of alcohol (100%, 80%, 70%) for three minutes each and then into water, stained in Harris' hematoxylin solution for 5 minutes and washed in running water. They were differentiated in 1% acid alcohol and then washed well in water, blued in Scott's tap water substitute for 5 minutes and rinsed briefly in distilled water, counterstained in 1% aqueous eosin for 2 minutes, washed well in water, dehydrated in descending grades of alcohol, cleared in xylene and mounted in DPX (Destrene, plasticiser and xylene). Sections were then placed in slide carriers and placed in a 400C oven to dry overnight. They were read microscopically.

Data Analysis

Data was analyzed using one-way ANOVA, followed by Duncan post hoc test (SPSS version 23). Results are presented as mean ± standard deviation of means obtained (n=5) with significance at $p < 0.05$.

RESULTS AND DISCUSSION

4 Characterization of Ferrous Nanoparticles

4.1.4.1 Spectrophotometric determination of $FeCl_3$ reduction

In this study, ferrous nanoparticles were synthesized from *Psidium guajava* leaf. Exactly, five different peaks were observed which include: 200nm, 300nm, 320nm, 340nm and 360nm respectively. The highest absorption characteristic peak of the ultraviolet-visible spectrum of the ferrous nanoparticles was observed at 360nm (Figure 4.3)

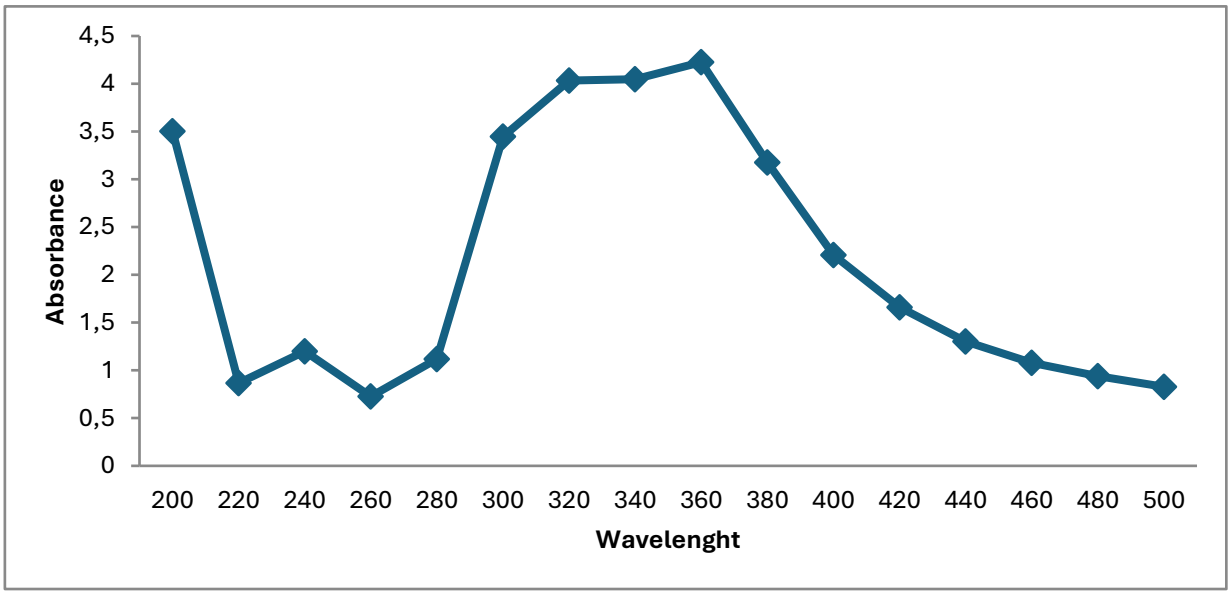

Fig 4.3: Characterization Biosynthesized Ferrous Nanoparticles from *Psidium guajava* Leaf Using UV-Visible Spectroscopy

4.1.4.2 FTIR spectroscopy characterization of green synthesized ferrous nanoparticles

The crystal of green synthesized ferrous nanoparticles produced was subjected to FTIR spectroscopy for its characterization. The FTIR characterization different spectra and absorbance bands which have been observed in the region of 3417.01 cm−1, 2923.22 cm−1, 1648.23 cm−1, 1412.90 cm−1, 1154.43 cm−1, 1034.84 cm−1, 675.11 cm−1, 596.02 cm−1 and 419.53 cm−1 which indicate O-H group, alkane (C-H) group, alkene (C=C) group, alkane (C-H) group, Alcohols (C-O) group, Aromatic compounds (C-H out-of-plane bending), alkyl Bromide (C-Br) and alkyl iodide (C-I) respectively. The changes

observed in the reaction converting $FeCl_3$ to FeNPs using FTIR analysis is represented below (Figure 4.4).

Table 4.4: FTIR Spectroscopy Showing the Wavelength, Functional Groups and Inference.

S/N	WAVENUMBER (cm^{-1})	FUNCTIONAL GROUPS	INFERENCES
1	3417.01	O-H stretch	Hydroxyl group (Found alcohols and phenol
2	2923.22	C-H stretch	Alkanes
3	1648.23	C=C stretch	Alkenes
4	1412.90	C-H bending	Alkanes
5	1154.43	C-O stretch	Alcohols, ethers, Carboxylic acids and esters
6	1034.84	C-O stretch	Alcohols, ethers, Carboxylic acids and esters
7	675.11	C-H stretching out of plane bending	Aromatic compound
8	596.02	C-Br stretching	Alkyl bromides
9	419.53	C-I stretching	Alkyl iodides

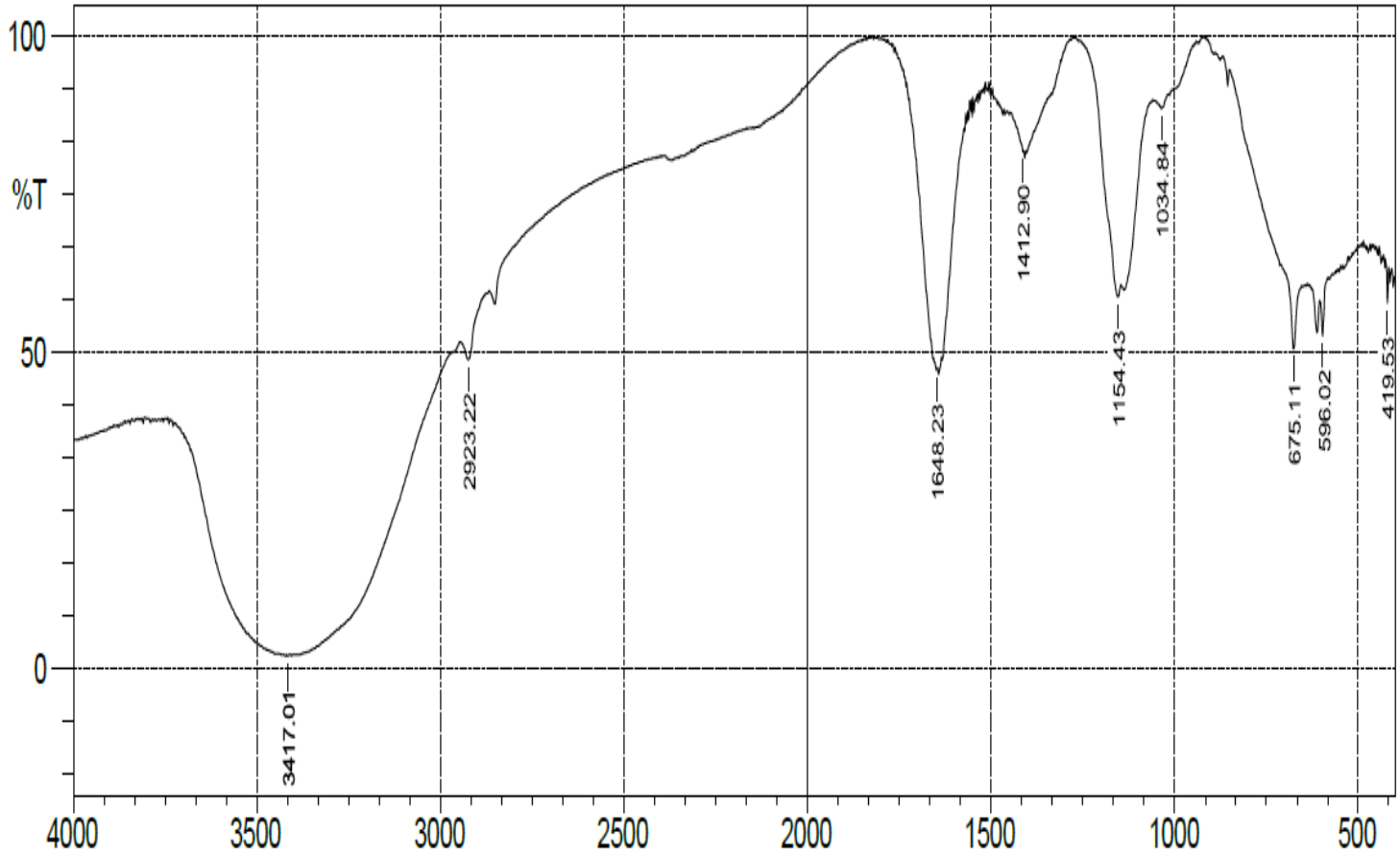

Fig 4.4: FT-IR Spectrum of Ferrous Nanoparticles Synthesised from *Psidium guajava* Leaf Extract

4.1.4.3 Characterization of ferrous nanoparticles using GC-MS

The characterization of ferrous nanoparticles (FeNPs) synthesized using *Psidium guajava* leaf extract was performed via Gas Chromatography-Mass Spectrometry (GC-MS). The analysis revealed various phytoconstituents which include: n-Hexadecanoic acid 29.82% ($C_{16}H_{32}O_2$), Oleic acid 27.37% ($C_{18}H_{34}O_2$), 2-Methoxy-4-vinylphenol 1.64% ($C_9H_{10}O_2$), Cyclopropanecarboxylic acid 5.10% ($C_{11}H_{12}O_2$), Undecanoic acid 4.37% ($C_{11}H_{22}O_2$), Myristic acid 3.39% ($C_{14}H_{28}O_2$), Erucic acid 4.67% ($C_{22}H_{42}O_2$) Oxacyclododecan-2-one (Lactone) 4.91% ($C_{11}H_{20}O_2$), Octadecanoic acid 15.15% ($C_{18}H_{36}O_2$), 9,12-octadecadienoic acid 1.30% ($C_{18}H_{32}O_2$), Eicosanoic acid 1.51% ($C_{20}H_{40}O_2$), Squalene 0.78% ($C_{30}H_{50}$), and their respective area percentages listed in Table 4.5. Among these, n-Hexadecanoic acid (29.82%) and Oleic acid (27.37%) were predominant, indicating their significant presence in the biosynthesized ferrous nanoparticles.

Table 4.5: GC-MS of Biosynthesized Ferros Nanoparticles from *Psidium guajava* leaf

S/N	Compound	Retention Time	Area%	Chemical formula
1	2-Methoxy-4-vinylphenol	08.319	01.640	$C_9H_{10}O_2$
2	Cyclopropanecarboxylic acid	08.983	05.100	$C_{11}H_{12}O_2$
3	Undecanoic acid	11.798	04.370	$C_{11}H_{22}O_2$
4	Myristic acid	14.189	03.390	$C_{14}H_{28}O_2$
5	Oxacyclododecan-2-one (Lactone)	17.427	04.910	$C_{11}H_{20}O_2$
6	n-Hexadecanoic acid	17.831	29.820	$C_{16}H_{32}O_2$
7	Erucic acid	19.303	04.670	$C_{22}H_{42}O_2$
8	Oleic acid	20.667	27.370	$C_{18}H_{34}O_2$
9	Octadecanoic acid	20.941	15.15	$C_{18}H_{36}O_2$
10	9,12-octadecadienoic acid	21.700	01.300	$C_{18}H_{32}O_2$
11	Eicosanoic acid	23.233	01.510	$C_{20}H_{40}O_2$
12	Squalene	27.736	00.780	$C_{30}H_{50}$

Extract

Fig 4.5: GC-MS Chromatogram of Biosynthesized Ferrous Nanoparticles from *Psidium guajava* Leaf

4.1.5 Effects of Green Synthesised Ferrous Nanoparticles on Liver Function Parameters

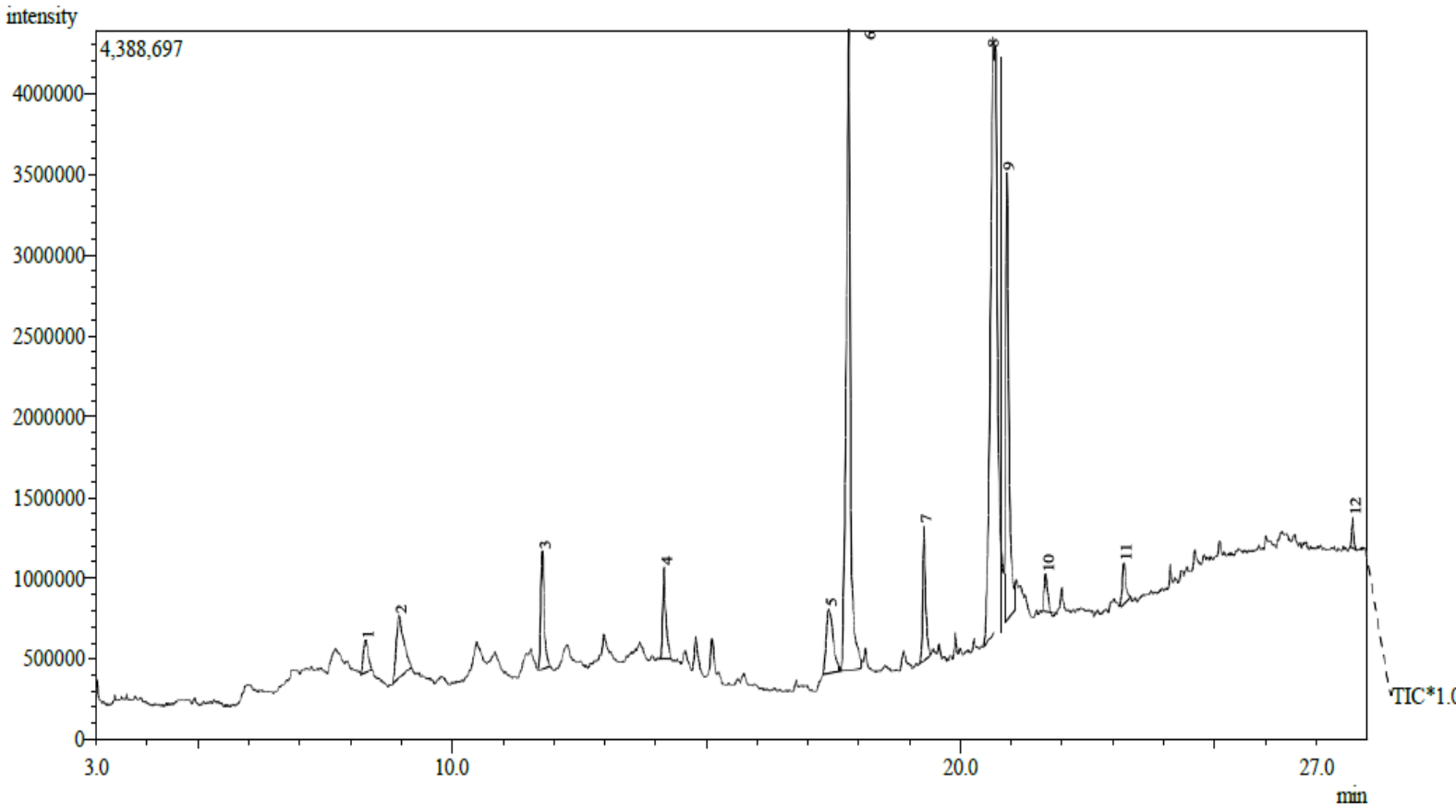

The result for ALP in Table 4.6 showed that there was no statistical significant difference (P > 0.05) between groups 1 and 3. However, there was significant differences (P <0.05) between groups 2, 4 and group 5 when compared with the control. The result of AST in group 2 showed no significantly difference (P <0.05) when compared to the control group. However, there were significant differences (P < 0.05) between groups 3, 4 and 5 when compared with the control (group 1). The result for ALT showed significantly differences in all the treated groups when compared with control. The result for ALB showed significantly differences in all the treated groups when compared to group 1. There were non-significant difference (P > 0.05) in TB, DB, and IDB levels between the control group and group 2. However, administration of 250, 500, and 1000mg/kg (group 3-5) caused significant (P > 0.05) increases in TB and IDB levels compared to the control. Notably, DB levels showed non- significant difference between group 2 and 3 when compared to the control group but showed a significant increase (P <0.05) between groups 4 and 5 when compared to the control group. The result for TP showed no statistical significant difference (P > 0.05) between groups 1 and 2. However, there was significance differences (P <0.05) between group 3, 4 and 5 when compared with group 1.

Table 4.6: Serum Levels of Selected Liver Function Parameters of Male *Wistar* Rats Administered Ferrous Nanoparticles Synthesized from *Psidium guajava* Leaf

Parameters	Group 1 Normal control	Group 2 (100 mg/Kg b.w)	Group 3 (250 mg/Kg b.w)	Group 4 (500 mg/Kg b.w)	Group 5 (1000 mg/Kg b.w)
ALP (U/L)	33.68 ± 0.60^{a}	34.85 ± 0.86^{b}	33.31 ± 0.78^{a}	40.06 ± 0.14^{d}	36.33 ± 1.38^{d}
AST (U/L)	51.48 ± 1.16^{a}	51.80 ± 0.84^{a}	59.00 ± 0.00^{b}	76.40 ± 0.89^{c}	89.00 ± 0.00^{d}
ALT (U/L)	48.36 ± 0.81^{c}	33.20 ± 1.21^{a}	42.82 ± 0.59^{b}	41.2 ± 2.05^{b}	50.80 ± 1.79^{d}
ALB (g/dL)	4.83 ± 0.11^{b}	6.39 ± 0.34^{c}	4.37 ± 0.17^{a}	4.08 ± 0.07 ^{a}	4.35 ± 0.24^{a}
TB (mg/dL)	0.95 ± 0.12^{a}	0.95 ± 0.14^{a}	1.61 ± 0.25^{b}	1.97 ± 0.21^{b,c}	2.29 ± 0.78^{c}
DB (mg/dL)	0.06 ± 0.03^{a}	0.08 ± 0.05^{a}	0.07 ± 0.04^{a}	0.52 ± 0.20^{b}	0.72 ± 0.42^{b}
IDB (mg/dL)	0.89 ± 0.13^{a}	0.87 ± 0.14^{a}	1.54 ± 0.22^{b}	1.45 ± 0.22^{b}	1.57 ± 0.39^{b}
TP (g/dL)	5.52 ± 0.16^{c}	4.91 ± 0.63^{b,c}	4.34 ± 0.30^{b}	6.82 ± 0.84^{d}	3.34 ± 0.22^{a}

Results are expressed as mean ± standard deviation of groups results obtained (n=5)

Mean values ± standard deviation in the same row with different letter of the alphabet as superscript showed statistically significant different ($p<0.05$).

Legend: ALP= Alkaline phosphatase, AST= Aspartate Aminotransferase, ALT= Alanine aminotransferase, ALB= Albumin, TB= Total bilirubin, DB= Direct bilirubin, INB= Indirect bilirubin, TP= Total protein.

4.1.6 Effects of Green Synthesized Ferrous Nanoparticles from Psidium guajava Leaf on Lipid Peroxidation and In-vivo Antioxidant Enzymes.

The results for MDA in Table 4.7 showed no statistical differences ($p > 0.05$) in all the treated groups. Apparently, there was increased in all the treated groups when compared to the control group. The result for CAT showed significant differences in all the treated groups. Apparently, there were increased in all the treated groups except group 2 that showed decrease when compared to the control group. The result for SOD showed no significance differences in group 2 and 3 when compared with the control group. However, there were significant differences in groups 4 and 5 when compared with group 1.

Table 4.7 Lipid Peroxidation and *In-vivo* Antioxidant Enzymes of Male Wistar Rats Administered Ferrous Nanoparticles Synthesized from *Psidium guajava* Leaf

Parameters	**GROUP 1 (Control)**	**GROUP 2 (100ppm B.W)**	**GROUP 3 (250ppm B.W)**	**GROUP 4 (500ppm B.W)**	**GROUP 5 (1000ppm B.W)**
MDA (μM)	1.06 ± 0.00[a]	2.82 ± 0.38[a]	2.01 ± 1.29 [a]	1.33 ± 0.03 [a]	3.81 ± 2.30 [a]
AT (U/mg)	145.58 ± 0.69[b]	124.6 ± 0.35 [a]	166.38 ± 1.47[c]	168.16 ± 1.77 [c]	188.75 ± 1.12[d]
SOD (U/mL)	3.28 ± 0.83[a]	3.55 ± 0.65[a]	3.53 ± 0.76[a]	18.61 ± 0.69[b]	18.80 ± 2.36[b]

Results are expressed as mean ± standard deviation of group result obtained (n=5)

Mean values ± standard deviation in the same row with different letters of the alphabets as superscript shows statistically significant difference ($p < 0.05$).

Legend: MDA= Malondialdehyde, SOD= Superoxide dismutase, CAT= Catalase

4.1.7: Histological Examination of Male Wistar Rats Liver Tissues Administered with Green Synthesized Ferrous Nanoparticles

The photomicrographs below showed that the administration of ferrous nanoparticles at various dose concentrations causes alteration in the normal liver architecture (Plate 2-5).

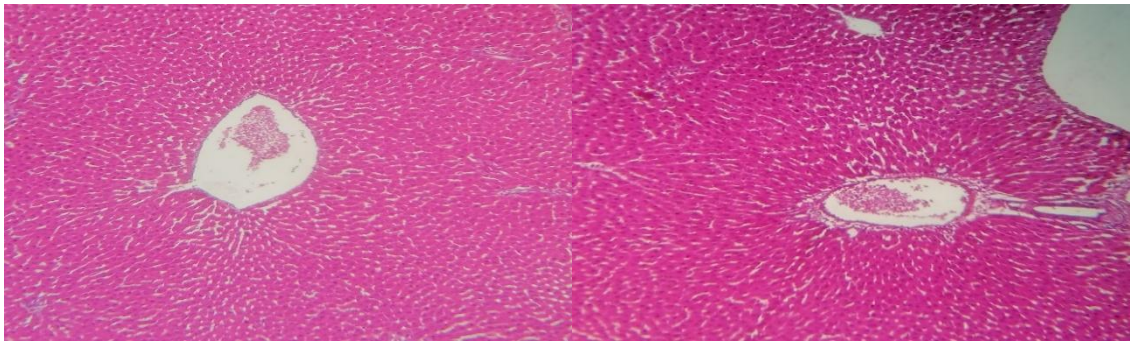

Plate 1: Photomicrograph of liver Section of Control Group Rats

Liver of wistar rats exposed to normal environmental and nutritional condition, showing normal architecture as shown by clear capsular space. No pathology observed. Stain: Hematoxylin and eosin Magnification ×100

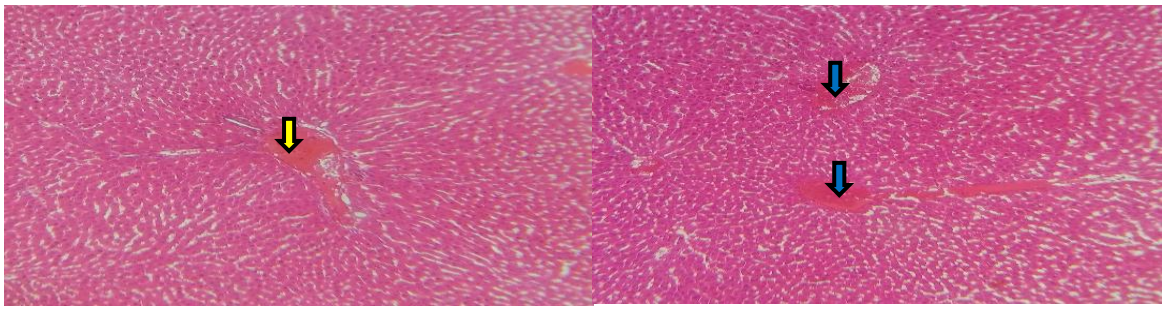

Plate 2: Photomicrograph of Liver Section of Group 2 Rats

Liver of wistar rat treated with 100ppm FeNps, exhibited congestion of the portal vein as indicated by the yellow arrow and the central vein as indicated by the blue arrows.

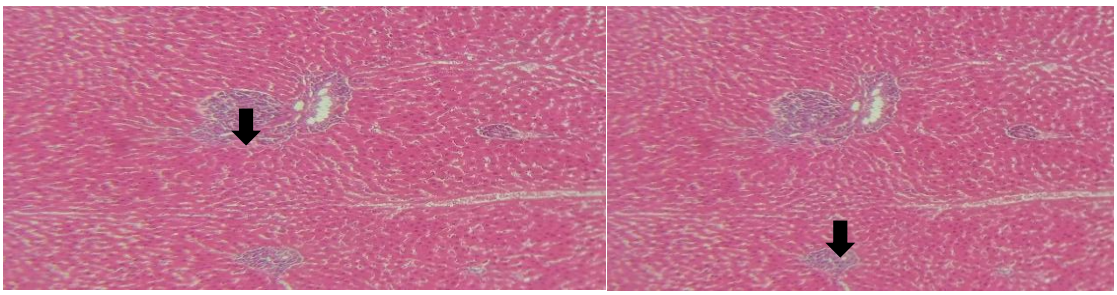

Plate 3: Photomicrograph of Liver Section of Group 2 Rats

Liver of wistar rat treated with 100ppm FeNps, exhibited aggregation of polymorphonuclear cells (white blood cells) indicated by the black arrows. This could indicate an infection.

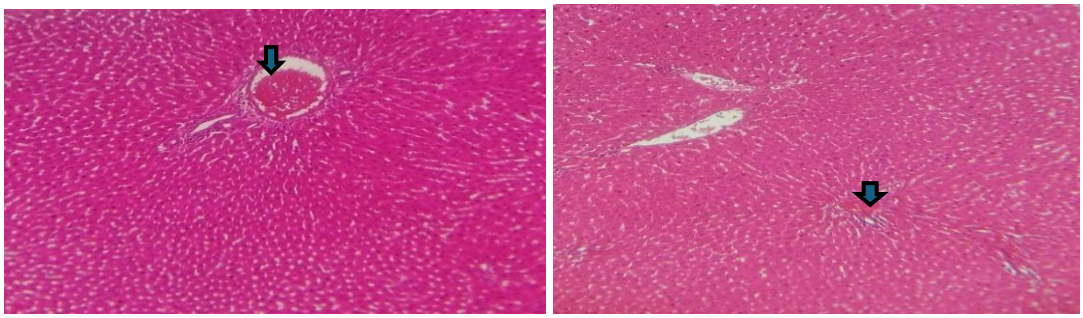

Plate 4: Photomicrograph of Liver Section of Group 3 Rat

Liver of wistar rat treated with 250ppm FeNps, exhibited congestion of the portal vein indicated by the blue arrows.

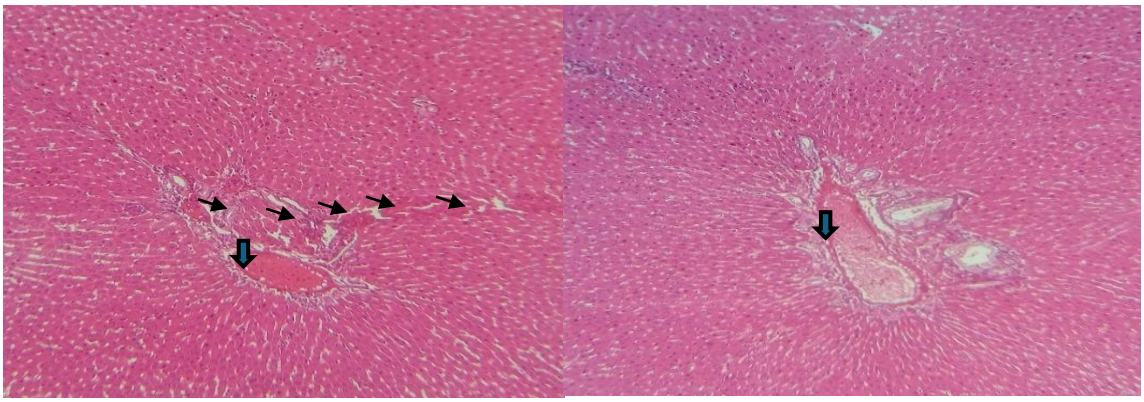

Plate 5: Photomicrograph of Liver Section of Group 4 Rats

Liver of wistar rat treated with 500ppm FeNps, exhibited congestion of the portal vein indicated by the blue arrows and necrosis of the hepatocytes as indicated by the back arrows.

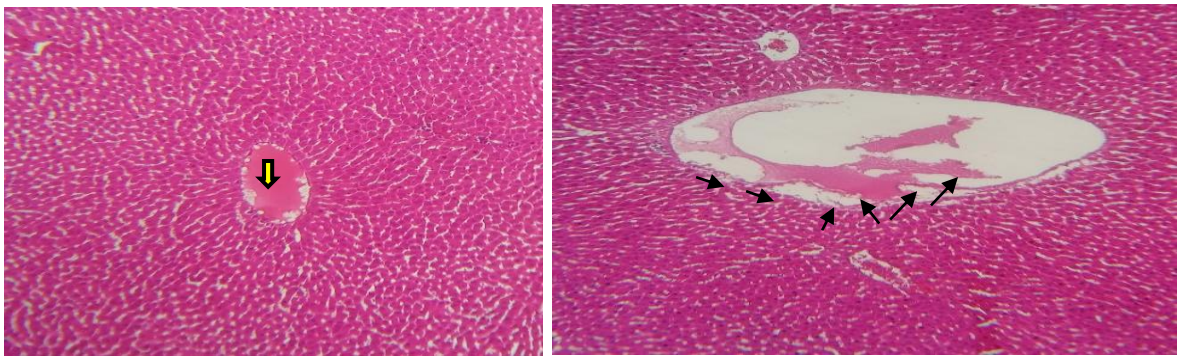

Plate 6: Photomicrograph of Liver Section of Group 5 Rats

Liver of wistar rat treated with 1000ppm FeNps, exhibited congestion of the central vein indicated by the yellow arrow and severe necrosis of the hepatocytes and the wall of the central vein as indicated by the back arrows.

DISCUSSION

The Characterization of Ferrous Nanoparticle by UV- visible spectroscopy: FeNPs was prepared via green route using *Psidium guajava* leaf (Fig. 4.5) extracts at room temperature. The absorption spectrum of FeNPs is shown in Fig. 4.5 and the peak observed at 360 nm was an indication of FeNPs, which is in accordance with already reported study (Behera *et al.,* 2012). The result obtained in Figure 4.5 illustrates the

formation and stability of FeNPs from their respective salts which gives characteristic peaks at different wavelengths using UV-visible spectroscopy. Optical properties of synthesized nanoparticles were analyzed by using UV-visible spectroscopy. UV-visible spectroscopy gives the optical properties of the nanomaterial in the form of absorbance peaks. UV-visible spectra of prepared nanoparticles which are produced by the guava leaf are shown in Figure 4.5 by adding extract with iron solution, $Fe3^{+}$ ion reduced to Fe^{2+} ions indicated by the UV-visible spectroscopy. Due to excitation of electrons, color of the solution changes. By adding the iron solution with the extract, color of the solution has been changed due to surface plasmon resonance (SPR) (Malik *et al.,* 2015). The color changes immediately after adding the plant extract to the iron salt solution confirmed the formation of FeNPs. In a matter of seconds, the color of the mixture changed from transparent yellow to black, demonstrating the synthesis of iron nanoparticles. The FeNPs dark colour was caused by surface Plasmon excitation vibrations, which is in accordance with the study conducted by Devatha *et al.* (2016).

Characterization of Ferrous Nanoparticles by FTIR

The FT-IR analysis was carried out to determine the molecules and/or functional groups that were present in the biosynthesized ferrous nanoparticles from guava leaf. Figure 4.6 shows the spectra of FeNP with peaks between 3417.01cm-1 and 419.53cm-1. FeNPs spectra and absorbance bands have been observed in the region of 3417.01, 2923.22, 1648.23, 1412.90, 1154.43, 1034.84, 675.11, 596.02 and 419.53 cm−1 which indicate O-H group, alkane (C-H) group, alkene (C=C) group, alkane (C-H) group, Alcohols (C-O) group, Aromatic compounds (C-H out-of-plane bending), alkyl Bromide (C-Br) and alkyl iodide (C-I) respectively. The strong broad absorption peak at 3417.01cm-1 is assigned to O-H stretching of carboxylic acid; and the peak at 419.53cm-1 is assigned to C-I stretching of alkyl iodide. FTIR identifies various groups that involve the reduction and capping of NPs. FTIR spectroscopy measures the spectral peaks of functional groups. The band at 3417.01 cm^{-1} may be due to (O-H stretch) this peak indicates the presence of hydroxyl groups, or phenolic groups, which are commonly found in alcohols and phenols (Sivakami *et al.,* 2021). The broad nature of this peak suggests strong hydrogen bonding, which is typical in such compounds. This finding accords with studies that reported hydroxyl groups on the surface of iron oxide nanoparticles, enhancing their hydrophilicity and reactivity. O-H stretching of polyphenol compounds causes peaks to appear between 3300 cm-1 and 3500 cm-1 (Jeyasundari *et al.,* 2017; Liu *et al.,* 2018; Pan *et al.,* 2020). The

reduction of ferric chloride and its aqueous phase is mostly due to phenolic chemicals (Kanagasubbulakshmi and Kadirvelu, 2017). Plant extracts include phenolic compounds, which are well-known for functioning as reducing agents (Devatha *et al.,* 2016; Pan *et al.,* 2020). They additionally serve as stabilizers by strengthening connections with water molecules (Jeyasundari *et al.,* 2017; Farshchi *et al.,* 2018). The FTIR analysis of FeNPs suggested that they might be surrounded by any of these organic molecules such as polyphenols, alkaloids and terpenoids, Kalainila *et al.* (2014) had already reported similar of results. The chemical constituents present in plant leaves extract such as flavonoids, alkaloids and fatty acids are responsible for the reduction of ferric ions to ferrous nanoparticles due to their capping and reducing capacity.

Characterization of Ferrous Nanoparticles by GC-MS

The characterization of ferrous nanoparticles (FeNPs) synthesized using *Psidium guajava* leaf extract was carried out using Gas Chromatography-Mass Spectrometry (GC-MS). The analysis identified various phytoconstituents, with notable compounds and their respective area percentages detailed in Table 4.5. Among these, n-Hexadecanoic acid (29.82%) and Oleic acid (27.37%) were the predominant compounds, indicating their significant presence in the synthesized nanoparticles. Predominant compounds n-Hexadecanoic acid 29.82% ($C_{16}H_{32}O_2$), Oleic acid 27.37% ($C_{18}H_{34}O_2$), while other identified compounds 2-Methoxy-4-vinylphenol 1.64% ($C_9H_{10}O_2$), Cyclopropanecarboxylic acid 5.10% ($C_{11}H_{12}O_2$), Undecanoic acid: 4.37% ($C_{11}H_{22}O_2$), Myristic acid 3.39% ($C_{14}H_{28}O_2$), Oxacyclododecan-2-one (Lactone) 4.91% ($C_{11}H_{20}O_2$), Octadecanoic acid 15.15% ($C_{18}H_{36}O_2$), 9,12-octadecadienoic acid 1.30% ($C_{18}H_{32}O_2$), Eicosanoic acid 1.51% ($C_{20}H_{40}O_2$), Squalene 0.78% ($C_{30}H_{50}$). The presence of n-Hexadecanoic acid and Oleic acid in significant amounts suggests that these fatty acids may play a crucial role in the stabilization and functionalization of the synthesized FeNPs. Fatty acids are known to enhance the biocompatibility and stability of nanoparticles, which is essential for their application in various fields, including medicine and environmental science. The characterization of ferrous nanoparticles using GC-MS has been documented in various studies, highlighting the importance of plant extracts in nanoparticle synthesis. For instance, studies have shown that plant-derived compounds, particularly fatty acids, can significantly influence the size, shape, and stability of nanoparticles (Wang *et al.,* 2024). The findings from this study align with previous research that identified similar fatty acids in nanoparticles synthesized from other plant extracts, indicating a commonality in the phytochemical profiles that contribute

to nanoparticle formation (Saar and Brysch, 2020). Moreover, the use of *Psidium guajava* leaf extract for synthesizing nanoparticles has been noted for its rich phytochemical content, which not only aids in the reduction of metal ions but also provides a stabilizing effect on the resulting nanoparticles. This reinforces the potential of guava leaves as a sustainable resource for nanoparticle synthesis, contributing to green chemistry practices. These findings are consistent with existing literature, underscoring the role of plant extracts in the synthesis and stabilization of nanoparticles.

Liver Function Parameter

The liver is the site of major metabolic processes in the body, including detoxification of blood, production of bile for the breakdown of fats in the digestive track, the storage of glucose in the form of glycogen, and the synthesis of amino-acid precursors that make up proteins (Njoku, 2014). And again, the liver is the largest internal organ in the human body, weighing about 1.5kg and accounting for about 2 to 3% of an adult's total body weight (Skandalakis *et al.*, 2004; Howida, 2016). Nanoparticles/nanomaterials have been known to enter systemic circulation. Therefore, they have the potential to cause organ damage throughout the body. The organs with extensive blood supply such as liver, spleen and kidneys are especially vulnerable. The serum levels of liver function biomarkers in male Wistar rats administered ferrous nanoparticles synthesized from *Psidium guajava* leaf are presented in Table 4.6. The parameters assessed were ALP, AST, ALT, ALB, TB, DB, IDB, and TP. The study evaluated the effects across five experimental groups, with Group 1 serving as the normal control and Groups 2 to 5 receiving increasing doses (100–1000 mg/kg b.w) of the nanoparticles.

Alkaline Phosphatase (ALP)

ALP levels in the control group were 33.68 ± 0.60 U/L. Treated groups showed a non-significant increased, peaking at 40.06 ± 0.14 U/L in Group 4 (500 mg/kg) and slightly decreasing in Group 5 (1000 mg/kg). Although these increases were modest, they may suggest mild hepatobiliary stress or early signs of cholestasis, particularly at intermediate doses. Elevated ALP can be associated with biliary obstruction or hepatic cell membrane damage.

Aspartate Aminotransferase (AST) and Alanine Aminotransferase (ALT)

AST showed a progressive and dose-dependent increase from 51.48 ± 1.16 U/L in the control to 89.00 ± 0.00 U/L in Group 5. A similar trend, though less consistent, was

observed in ALT levels, which reached 50.80 ± 1.79 U/L in Group 5 compared to 48.36 ± 0.81 U/L in the control. The highest levels of these enzymes at 1000 mg/kg indicate marked hepatocellular injury. These enzymes, particularly ALT, are reliable indicators of liver damage due to their high concentration in hepatocytes. Elevated levels signify increased permeability or rupture of hepatocellular membranes.

Albumin (ALB)

Serum albumin concentration significantly increased in Group 2 (6.39 ± 0.34 g/dL), suggesting a possible stimulatory effect of low-dose nanoparticles on liver synthetic function. However, at higher doses, especially in Group 5 (4.35 ± 0.24 g/dL), albumin levels declined below control levels, indicating impaired protein synthesis. This decline may reflect a reduction in liver biosynthetic capacity or damage to hepatocytes responsible for albumin production.

Total Bilirubin (TB), Direct Bilirubin (DB), and Indirect Bilirubin (IDB)

Bilirubin is a sensitive marker of liver functions, and its elevation indicates hepatocellular injury or biliary obstruction (Yao *et al.*, 2020). The significant increase in total and indirect bilirubin in rats exposed to 250–1000 mg/kg of nanoparticles suggests that ferrous nanoparticles at these concentrations may disrupt hepatocyte integrity or impaired the conjugation process in the liver, leading to an accumulation of unconjugated bilirubin in the blood. The elevated direct bilirubin levels at 500 and 1000 mg/kg further indicate the presence of cholestasis or damage to the bile canalicular membrane (Duhan *et al.*, 2017). This dose-dependent effect correlates with previous studies reporting nanoparticle-induced oxidative stress and membrane destabilization in hepatic tissues (Fuhan *et al.*, 2017). The absence of significant changes at 100 mg/kg implies a threshold below which the nanoparticles exert minimal toxic effects on bilirubin metabolism.

Overall, the pattern of increased TB, DB, and IDB at higher doses demonstrates the potential hepatotoxicity of green-synthesized ferrous nanoparticles, emphasizing the importance of dose regulation for biomedical applications.

Total Protein (TP)

Total proteins were significantly reduced in Groups 3 (4.34 ± 0.30 g/dL) and 5 (3.34 ± 0.22 g/dL) compared to the control, suggesting compromised synthetic function at these doses. Interestingly, TP peaked in Group 4 (6.82 ± 0.84 g/dL), possibly due to an

acute-phase response or inflammatory stimulation. Persistent reduction in protein levels at the highest dose further supports hepatic dysfunction, possibly indicating impaired synthesis or protein catabolism.

The findings demonstrate a dose-dependent hepatotoxic effect of ferrous nanoparticles synthesized from *Psidium* guajava leaf. The significant elevation of ALP, AST, ALT, TB, DB, and IDB at higher doses suggests progressive hepatocellular injury, while the reduction in albumin and total protein indicated impaired synthetic function. These biochemical interruptions bear clinical relevance, as similar patterns are observed in toxic hepatitis, drug-induced liver injury, and heavy metal nanoparticle overload in humans (singh *et al.*, 2019; khan *et al.*, 2020; Jaeschke *et al.*, 2021). The relatively stable enzyme levels at lower doses (Group 2) may imply a threshold of safety, beyond which the nanoparticles exert harmful effects. While ferrous nanoparticles from *Psidium guajava* show some biological activity at lower doses, their administration at higher concentrations (≥500 mg/kg) results in significant liver toxicity in male Wistar rats. These findings highlight the need for dose optimization and safety evaluation before considering any clinical or therapeutic application of such nanoparticles.

Lipid peroxidation Activity in Male Wistar Rats Liver Tissues Administered Ferrous Nanoparticles

This study investigated the oxidative stress and antioxidant response in Wistar rats administered various doses (100–1000 ppm) of a treatment with green-synthesized ferrous nanoparticles derived from *Psidium guajava* leaf extract. Key biomarkers analyzed include Malondialdehyde (MDA) as a marker of lipid peroxidation, and Superoxide Dismutase (SOD) and Catalase (CAT) as endogenous antioxidant enzymes.

The results demonstrated a dose-dependent biphasic response. At lower doses (100–250 ppm), there is a moderate increase in MDA, indicating mild oxidative stress. Interestingly, MDA significantly drops at 500 ppm, suggesting that this concentration may exert a protective or adaptive antioxidant effect. However, at the highest dose (1000 ppm), MDA sharply increases, indicating significant oxidative membrane damage likely due to nanoparticle-induced toxicity. Malondialdehyde (MDA) is a reactive aldehyde and a byproduct of lipid peroxidation, which occurs when reactive oxygen species (ROS) attack polyunsaturated fatty acids in cell membranes. It is commonly used as a biomarker of oxidative stress and cellular membrane damage. Elevated MDA levels are indicative of

increased lipid peroxidation and oxidative damage, and they are frequently observed in conditions such as toxic hepatitis, metal toxicity, and oxidative liver injury (Ayala *et al.*, 2014).These findings are also consistent with clinical presentations in drug-induced liver injury and toxic hepatitis, where elevated MDA and fluctuating antioxidant enzyme activities are commonly observed (Bhattacharyya *et al.*, 2014).

In contrast, SOD and Catalase activities progressively increase with dosage. This reflects a compensatory up-regulation of the antioxidant defense system in response to reactive oxygen species (ROS) generated by the ferrous nanoparticles. The elevation is most profound at 500 ppm and 1000 ppm, aligning with findings by Ogunyemi *et al.* (2019), who reported enhanced antioxidant activity following exposure to green-synthesized metal nanoparticles in rats. Superoxide dismutase (SOD) is a critical antioxidant enzyme that catalyzes the dismutation of superoxide radicals (O_2^-) into molecular oxygen (O_2) and hydrogen peroxide (H_2O_2). It serves as the first line of defense against ROS in nearly all living cells. Elevated SOD activity is an adaptive response to increased oxidative stress and serves to prevent damage to DNA, proteins, and lipids (McCord and Fridovich, 1969; Wu *et al.,* 2014). Whereas catalase is an antioxidant enzyme that breaks down hydrogen peroxide (H_2O_2), a potentially harmful byproduct of metabolism, into water and oxygen.

It works in synergy with SOD to protect cells from oxidative damage. High levels of catalase indicate a robust antioxidant response but may also reflect a high oxidative load where detoxification is actively ongoing (Chelikani *et al.*, 2004). The high catalase level at 1000 ppm, despite elevated MDA, suggests that the antioxidant system was overwhelmed, potentially due to excessive ROS. This phenomenon has been reported in previous studies on metal nanoparticle toxicity, including works by Ahmed *et al.* (2016) and Duhan *et al.* (2017), where higher concentrations caused oxidative damage despite enzymatic up regulation.

This study revealed that the administration of *Psidium guajava* leaf-derived ferrous nanoparticles exhibits dual effects on oxidative balance depending on the dose. While moderate doses (especially 500 ppm) appear to enhance the antioxidant defense system and minimize oxidative damage, high doses (1000 ppm) result in oxidative stress and potential toxicity, as evidenced by elevated MDA despite enzymatic activity.

CONCLUSION

The synthetic process involved the reduction of Fe^{3+} ions to Fe^{2} using the bioactive components of the leaf extract, confirmed through UV-visible spectroscopy, Fourier Transform Infrared (FTIR) spectroscopy, and also using GC-MS. The absorption characteristic peak of the ultraviolet-visible spectrum of the ferrous nanoparticles was observed at 360nm. FTIR spectroscopy further characterized the synthesized nanoparticles, revealing prominent absorption peaks associated with functional groups such as hydroxyl (O-H), alkane (C-H), and alkene (C=C) groups. The strong O-H stretch at 3417.01 cm^{-1} suggested the presence of phenolic compounds in the extract, which are known for their reducing and stabilizing properties in nanoparticle synthesis. This analysis highlighted the role of organic molecules, including flavonoids and alkaloids, in the reduction of ferric ions to ferrous nanoparticles, thus establishing a chemical foundation for the therapeutic applications of FeNPs.

This study evaluated liver function biomarkers across five groups of wistar rats. These findings demonstrate a dose-dependent hepatotoxic effect of ferrous nanoparticles synthesized from *Psidium* guajava leaf. The significant elevation of ALP, AST, ALT, TB, DB, and IDB at high doses suggests progressive hepatocellular injury, while the reduction in albumin and total protein indicates impaired synthetic function.

This characterization of FeNPs revealed the highest absorption peak at 360nm observed in the UV-visible spectroscopy, Fourier transform infrared spectroscopy (FTIR) revealed the presence of functional biomolecules and crystal structure of FeNPs which contained some functional groups inference to be: hydroxyl (O-H), alkane (C-H), and alkene (C=C) among others. Further, characterization of the FeNPs was elicited by gas chromatography mass spectroscopy (GC-MS) showed 12 peaks which are of biological significance.

While ferrous nanoparticles from *Psidium guajava* show some biological activity at lower doses, their administration at higher concentrations (≥500 mg/kg) results in significant liver toxicity in male Wistar rats. These findings highlight the need for dose optimization and safety evaluation before considering any clinical or therapeutic application of such nanoparticles.

The results demonstrate a dose-dependent biphasic response. At lower doses (100–250 ppm), there is a moderate increase in MDA, indicating mild oxidative stress.

Interestingly, MDA significantly drops at 500 ppm, suggesting that this concentration may exert a protective or adaptive antioxidant effect. However, at the highest dose (1000 ppm), MDA sharply increases, indicating significant oxidative membrane damage likely due to nanoparticle-induced toxicity. In contrast, SOD and Catalase activities progressively increase with dosage. This reflects a compensatory up-regulation of the antioxidant defense system in response to reactive oxygen species (ROS) generated by the ferrous nanoparticles.

Histopathological examination of the rats' liver tissues revealed architectural alterations following exposure to green-synthesized ferrous nanoparticles in all treated groups. Control group exhibited normal liver architecture, characterized by clear capsular spaces (Plate 1). In contrast, liver of wistar rat treated with 100ppm to 500ppm FeNps, exhibited congestion of the portal vein as shown in (plate 2 to 4) and liver of wistar rats treated with 1000ppm FeNps, exhibited congestion of the central vein and severe necrosis of the hepatocytes and the wall of the central vein, severe necrosis coupled with vascular congestion at higher doses 1000 ppm (Plates 6). Notably, the 1000 ppm dose induced the most pronounced damage, suggesting a threshold for FeNP-induced hepatotoxicity.

Conflict of Interest

The authors affirm that there are no conflicts of interest associated with this publication.

Authors' Declaration

The authors confirm that the research presented in this article is entirely original. They accept full responsibility for any claims or issues arising from the content herein.

REFERENCE

Abbas, K., Saleh, A., Mohamed, A., MohdAzhan, N. (2009). The recent advances in nanotechnology and its applications in food processing: a review. *Food Agriculture Environment*, 7(**34**), 14–17.

Acharya, P., Chouhan, K., Weiskirchen, S., and Weiskirchen, R. (2021). Cellular mechanisms of liver Fibrosis. *Frontiers in Pharmacology*, 12, 1663-9812.

Aebi, H. E. (1983). Catalase. In H. U. Bergmeyer (Ed.): Methods of enzymatic analysis (pp. 273–286). Verlag Chemie.

Ahmed, S., Saifullah, Ahmad, M., Swami, B. L., & Ikram, S. (2016). Green synthesis of silver nanoparticles using Azadirachta indica aqueous leaf extract. *Journal of Radiation Research and Applied Sciences*, 9(**1**), 1–7.

Alberts, B., Johnson, A., Lewis, J., Raff, M., Roberts, K., and Walter, P. (2002). Protein function. in molecular biology of the cell, 4th edition, Garland Science: New York, NY, USA.

Anandharamakrishnan, C., Parthasarathi, S. (2019). Food nanotechnology: Principles and applications. CRC Press.

Arfat, Y., Arfat, N., Tahir, M. U., Rashid, M., Anjum, S., Zhao, F., and Qian, A. R. (2014). Effect of imidacloprid on hepatotoxicity and nephrotoxicity in male albino mice. *Toxicology Reports*, 1, 554-561.

Ariyarathna, I.R., Rajakaruna, R., Karunaratne, D.N. (2017). The rise of inorganic nanomaterial implementation in food applications. *Food Control*, 77, 251–259.

Arowora, K. A., Ugwuoke, K. C., Abah, M. A. and Ugwoke, B. C. (2023). Effects of green-synthesized silver nanoparticles from *Azadirachta indica* on growth performance and liver function parameters in male albino rats. *Cell Biology and Development*, 7(**1**), 28-34.

Arroyo-Maya, I.J., McClements, D.J. (2015). Biopolymer nanoparticles as potential delivery systems for anthocyanins: fabrication and properties. *Food Res. Int.* 69, 1–8.

Aryal, S. (2024). High performance liquid chromatography: principle, parts, types, uses, diagram. Microbes' notes. Retrieved from (URL).

Avella, M., Bruno, G., Errico, M., Gentile, G., Piciocchi, N., Sorrentino, A., Volpe, M. (2007). Innovative packaging for minimally processed fruits. *Packaging Technology Science International Journal*, 20(**5**), 325–335.

Avwioro, O. G. (2011). Histochemical uses of haematoxylin - A review. *Journal of Pharmacy and Clinical Sciences*, 1(**1**) 24-34.

Avwioro, O. G. (2011). Staining reactions of microwave-processed tissues compared with conventional paraffin wax-processed tissues. *European Journal of Experimental Biology*, 1(**1**), 57–62.

Ayala, A., Muñoz, M. F., and Argüelles, S. (2014). Lipid peroxidation: Production, metabolism, and signaling mechanisms of malondialdehyde and 4-hydroxy-2-nonenal. *Oxidative Medicine and Cellular Longevity,* 2014, 360438.

Barbara, K. and Nora, S. (2005). United States Environmental Protection Agency (US EPA) Proceedings: Nanotechnology and the Environment: Applications and Implications. Progress Review Workshop III, 1-8. Arlington, VA.

Behera, S. S., Patra, J. K., Pramanik, K., Panda, N., and Thatoi, H. (2012). Characterization and evaluation of antibacterial activities of chemically synthesized iron oxide nanoparticles. World *Journal of Nano Science and Engineering*, 2(**4**), 196–200.

Benjamin, M. B., Dennis, J. W., and Leonard, I. B. (2016). Disseminated intravascular coagulation. *American Journal of Clinical Pathology*, 146(**6**), 670-680.

Bhattacharyya, A., Chattopadhyay, R., Mitra, S., and Crowe, S. E. (2014). Oxidative stress: An essential factor in the pathogenesis of gastrointestinal mucosal diseases. *Physiological Reviews*, 94(**2**), 329–354.

Biswas, S., Talukdar, P. and Talapatra, D. S. N. (2019). Presence of phytochemicals in fruits and leaves of guava (*Psidium guajava* Linn.) for cancer prevention: A mini review. *J. Drug Deliv. Ther.*, 9, 726–729.

Bott, J., Stormer, A., Franz, R., 2014. A comprehensive study into the migration potential € of nano silver particles from food contact polyolefins. In: Chemistry of Food, Food Supplements, and Food Contact Materials: from Production to Plate. ACS Publications, pp. 51–70.

Bouwmeester, H., van der Zande, M., Jepson, M.A. (2018). Effects of food-borne nanomaterials on gastrointestinal tissues and microbiota. *Nanobiotechnology*, 10(**1**), 1481.

Braet, F., and Wisse, E. (2002) 'Structural and Functional Aspects of Liver Sinusoidal Endothelial Cell Fenestrae: A Review', Comparative Hepatology, 1(1), 1.

Cao, Y., Li, J., Liu, F., Li, X., Jiang, Q., Cheng, S., Gu, Y., 2016. Consideration of interaction between nanoparticles and food components for the safety assessment of nanoparticles following oral exposure: a review. Environ. Toxicol. Pharmacol. 46, 206–210.

Carneiro, C., Brito, J., Bilreiro, C., Barros, M., Bahia, C., Santiago, I., and Caseiro-Alves, F. (2019). All About Portal Vein: A Pictorial Display to Anatomy, Variants and Physiopathology. Insights into Imaging, 10(1), 38.

Chang, Y.C., Chen, D.H. (2005). Adsorption kinetics and thermodynamics of acid dyes on a carboxymethylated chitosan-conjugated magnetic nano-adsorbent. *Macromol. Bioscience*, 5(**3**), 254–261.

Chelikani, P., Fita, I., and Loewen, P. C. (2004). Diversity of structures and properties among catalases. *Cellular and Molecular Life Scienc*es, 61, 192–208.

Chellaram, C., Murugaboopathi, G., John, A., Sivakumar, R., Ganesan, S., Krithika, S., Priya, G., (2014). Significance of nanotechnology in food industry. APCBEE procedia 8, 109–113.

Choji T.P.P., Ngokere, A.A., Ogenyi, S.I., and Kumbish, P.R. (2015). Histo-architechtural evaluation of conventional versus two rapid microwave processing techniques. *British Biotechnology Journal* 8(**3**), 1-19.

Chung, C., and Iwakiri, Y. (2013). The lymphatic vascular System in liver diseases: Its role in ascites formation. *Clinical and Molecular Hepatology*, 19(**2**), 99-104.

Cruzat, V., Macedo, R. M., Noel, K. K., Curi, R., and Newsholme, P. (2018). Glutamine: Metabolism and Immune Function, Supplementation and Clinical Translation. *Nutrients*, 10(**11**), 1564.

Cullen, J. M., and Stalker, M. J. (2016). Liver and biliary System. Jubb, Kennedy and Palmer's Pathology of Domestic Animals, 1**(2**), 258-352.

Daniel, M., and Astruc, D. (2004). Gold nanoparticles: Assembly, Supramolecular chemistry, Quantum-Size-Related Properties, and Applications toward Biology, Catalysis, and Nanotechnology. *ChemInform,* 35(**16**), 234.

David. L., Moldovan, B., Vulcu, A., Olenic, L., Perde-Schrepler, M., FischerFodor, E., Florea, A., Crisan, M., Chiorean, I. and Clichici, S. (2014). Green synthesis, characterization and anti-inflammatory activity of silver nanoparticles using European black elderberry fruits extract. Colloids Surf B: *Biointerfaces*, 122, 767-777.

De Azeredo, H.M., (2009). Nanocomposites for food packaging applications. *Food Res. Int.* 42(**9**), 1240–1253.

De Francisco, E.V., García-Estepa, R.M., 2018. Nanotechnology in the agrofood industry. *Journal of Food Engineering*, 238, 1–11.

Devatha, C. P., Thalla, A. K., and Katte, S. Y. (2016). Green synthesis of iron nanoparticles using different leaf extracts for treatment of domestic wastewater. *Journal of Cleaner Production*, 139, 1425–1435.

Dianyuan, Z., Fengjiao, Y., Yang, W., Site, L., Yang, L., Fei, H., Wenting, Y., Di, L., Yuandong, T., Qian, L., Jing, W., Fuchu, H., and Li, T. (2022). ALK1 Signaling is required for the homeostasis of kupffer cells and prevention of bacterial infection. *The Journal of Clinical Investigation*, 132(**3**), 1-15.

Drago, E., Campardelli, R., Pettinato, M., Perego, P. (2020). Innovations in smart packaging concepts for food: an extensive review. *Foods* 9(**11**), 1628.

Duhan, J.S., Kumar, R., Kumar, N., Kaur, P., Nehra K. and Duhan, S. (2017). Nanotechnology: the new perspective in precision agriculture, a review article. *Biotechnology Report,* 1(**5**), 11- 23

Duncan, T.V. (2011). Applications of nanotechnology in food packaging and food safety: barrier materials, antimicrobials and sensors. *Journal of Colloid Interface Science*, 363(**1**), 1–24.

Dutta, P., Kundu, S., Bauri, F. K., Talang, H., and Majumder, D. (2014). Effect of bio-fertilizers on physico-chemical qualities and leaf mineral composition of guava grown in alluvial zone of West Bengal. *Journal of Crop Weed*, 10, 268–271.

Dutta, S., Mishra, S. P., Sahu, A. K., Mishra, K., Kashyap, P., and Sahu, B. (2021). Hepatocytes and their role in metabolism. In (Ed.), Drug Metabolism. IntechOpen, 1-9.

Eesha, B. R., Mohanbabu, A. V., Meena, K. K., Vijay, M., Lalit, M., and Rajput, R. (2011). Hepatoprotective activity of Terminalia paniculata against paracetamol induced hepatocellular damage in wistar albino rats. *Asian Pacific Journal of Tropical Medicine*, 4(**6**), 466-469

Egwaoje, M., Aigbiremolen, A. A., Ativie, R. N., Ohwin, P. E., Aromose, I. K., Odigie, M. O., and Igweh, J. C. (2017). Alterations of aqueous *Persea americana* seed extract on renal functions associated with diabetes mellitus in *Wistar* rats. *Journal of Advances in Medicine and Medical Research*, 24(**8**), 1–8.

Eidenberger, T., Selg, M. and Krennhuber, K. (2013). Inhibition of dipeptidyl peptidase activity by flavonol glycosides of guava (*Psidium guajava* L.): A key to the beneficial effects of guava in type II diabetes mellitus. *Fitoterapia* , 89, 74–79.

El-Ahmady, S. H., Ashour, M. L. and Wink, M. (2013). Chemical composition and anti-inflammatory activity of the essential oils of *Psidium guajava* fruits and leaves. *J. Essent. Oil Res.*, 25, 475–481.

Embgenbroich, M., and Burgdorf S. (2018). Current concepts of antigen cross presentation. *Frontiers in Immunology*, 9, 1664-3224.

Fathi, M., Donsi, F., McClements, D.J., (2018). Protein-based delivery systems for the nanoencapsulation of food ingredients. *Compr. Rev. Food Sci. Food Saf.* 17(**4**), 920–936.

Friedman, L. S., Martin, P., and Munoz, S. (2003). Laboratory evaluation of the patient with liver disease. Hepatology. WB Saunders, Philadelphia, PA, 671.

Fu, S., Wu, D., Jiang, W., Li, J., Long, J., Jia, C., and Zhou, T. (2020). Molecular biomarkers in drug-induced liver injury: Challenges and future perspectives. *Frontiers in Pharmacology*, 10, 1667.

Fuhan, L., Zhang, S., Zhang, S., and Liu, J. (2017). The effects of nanoparticles on liver biomarkers and histopathology. *Journal of Nanomedicine Research*, 5(**5**), 00130.

Gómez, A. A. J., Tapias, M., and Lúquez, M. A. (2020). Diagnostic and therapeutic approach for cholestasis in adulthood. *Revista Colombiana de Gastroenterología*, 35(**1**), 76-86.

Hansen, T. W. R., Wong, R. J., and Stevenson, D. K. (2020). Molecular physiology and pathophysiology of bilirubin handling by the blood, liver, intestine, and brain in the newborn. *American Physiological Society*, 100(**3**), 1291-1346.

Hassan, T. D. V., Naseer, I. and N, A. (2019). hepatoprotective activity of some medicinal plants: a review. *International Research Journal of Pharmacy*, 10(**5**), 9-16.

Hirn, S., Semmler-Behnke, M., Schleh, C., Wenk, A., Lipka, J., Schäffler, M., Takenaka, S., Möller, W., Schmid, G., Simon, U., and Kreyling, W. G. (2011). Particle size-dependent and surface charge dependent biodistribution of gold nanoparticles after intravenous administration. *European Journal of Pharmaceutics and Biopharmamaceutics*, 7(**7**), 407-416.

Hong, F., Wu, N., Zhou, Y., Ji, L., Chen, T., Wang, L., 2017. Gastric toxicity involving alterations of gastritis-related protein expression in mice following long-term exposure to nano TiO2. *Food Res. Int.* 95, 38–45.

Hoseinnejad, M., Jafari, S.M., Katouzian, I. (2018). Inorganic and metal nanoparticles and their antimicrobial activity in food packaging applications. *Crit. Rev. Microbiol.* 44**(2**), 161–181.

Howida, S. A. S. (2016). Physiological changes due to hepatotoxicity and the protective role of some medicinal plants. *Beni-suef University Journal of Basic and Applied Sciences*, 5(**3**), 134-146.

Hu, X. F., Zhang, Q., Zhang, P. P., Sun, L. J., Liang, J. C., Morris-Natschke, S. L., Chen, Y. and Lee, K. H. (2018). Evaluation of in vitro/in vivo anti-diabetic effects and identification of compounds from Physalis alkekengi. *Fitoterapia*, 127, 129–137.

Hudert, C. A., Tzschätzsch, H., Rudolph, B., Loddenkemper, C., Holzhütter, H. G., and Kalveram, L. (2021). How histopathologic changes in pediatric nonalcoholic fatty liver disease influence in vivo liver stiffness. *Acta biomaterialia*. 123, 178-186.

Hundt M, Basit H, John S. (2022). Physiology, bile secretion. Updated on sept.In: StatPearls, StatPearls Publishing.

Ibukuro, K., Fukuda, H., Tobe, K., Akita, K., and Takeguchi, T. (2016). The vascular anatomy of the ligaments of the liver: Gross anatomy, imaging and clinical applications. *The British Journal of Radiology*, 89(**1064**), 20150925.

Imo, C., and Imo, F. O. (2015). Phytochemical analysis of *Gongronema latifolium benth* Leaf using gas chromatographic flame ionization detector. *International Journal of Chemical and Biomolecular Science*, 1(**2**), 60-68.

Imo, C., Arowora, K. A., Ezeonu, C. S., Ikwebe, J., Yakubu, O. E., Imo, N. G., and Danlami, G. C. (2021). Biochemical and histological effects of ethanolic extracts of

fruits of xylopia aethiopica and seeds and leaves of Piper guineense on liver and kidney function in male albino rats. *Future Journal of Pharmaceutical Sciences*, 7, 1-12.

Imo, C., Zaku, J. S. (2019). Medicinal properties of ginger and garlic: A review. *Current Trends of Biomedical Engineering and Bioscience*, 18(**2**), 47-52.

Iqbal, A., Iqbal, K., Li, B., Gong, D., and Qin, W. (2017). Recent Advances in Iron Nanoparticles: Preparation, Properties, Biological and Environmental Application. *Journal of Nanoscience and Nanotechnology*, 17(**7**), 4386–4409.

Ishii, T., Seo, S., Ito, T., Ogiso, S., Fukumitsu, K., Taura, K., and Uemoto, S. (2020). Structure and surgical dissection layers of the bare area of the liver. *BMC surgery*, 20, 1-8.

Jaeschke, H., Ramachandran, A., and Chao, X. (2021). Mechanisms of drug-induced liver injury: Progress and challenges. *Current Opinion in Toxicology*, 2(**5**), 1–8.

Jeong, S. Y., Jin, H., and Chang, J. H. (2019). Crystal structure of L-aspartate aminotransferase from schizosaccharomyces pombe. *Plose One*, 14(**8**), 0221975.

Jesús, A. D. D. L., and Chad, R. B. (2020). Evaluation of oxidative stress in biological samples using the thiobarbituric acid reactive substances assay. *Journal of Visualized Experiments*, 15(**9**), 61155.

Jeyasundari, J., Praba, P. S., Jacob, Y. B. A., Vasantha, V. S., and Shanmugaiah, V. (2017). Green synthesis and characterization of zero valent iron nanoparticles from the leaf extract of *Psidium guajava* plant and their antibacterial activity. *Chemical Science Review and Letters*, 6(**24**), 1244–1252.

John, F. R., and Douglas, S. (2014). Hepatic structure and function. Gastrointestinal anatomy and physiology: *The Essentials*, 129-133.

Justin, F. C., Darren, M. G., David, E. S., and Terry, D. H. J. (2021). Bilirubin as a metabolic hormone: The physiological relevance of low levels. *American Journal of Physiology*, 3(**20**), 191-207.

Kalainila, P., Subha, V., Ernest Ravindran, R. S., and Renganathan, S. (2014). Synthesis and characterization of silver nanoparticle from *Erythrina indica*. *Asian Journal of Pharmaceutical and Clinical Research*, 7(**2**), 39–43.

Kalas, M. A., Chavez, L., Leon, M., Taweesedt, P. T., Surani, S. (2021). Abnormal liver enzymes: A review for clinicians. *World Journal of Hepatology*, 13(**11**), 1688-1698.

Kamimoto, K., Nakano, Y., Kaneko, K., Miyajima, A., and Itoh, T. (2020). Multidimensional imaging of liver injury repair in mice reveals fundamental role of the ductular reaction. *Communications Biology*, 3(**1**), 289.

Kanagasubbulakshmi, S., and Kadirvelu, K. (2017). Green synthesis of iron oxide nanoparticles using *Lagenaria siceraria* and evaluation of its antimicrobial activity. *Defence Life Science Journal*, 2(4): 422–427.

Keith, L. M., Arthur, F. D., and Anne, M. R. (2018). The liver synthesizes plasma proteins. clinically oriented anatomy 8th Edition, 1154

Khan, H. A., Abdelhalim, M. A. K., Alhomida, A. S., and Al Ayed, M. S. (2020). Effects of gold nanoparticles on hepatic tissue: A comparative study in rats. *Journal of Toxicologic Pathology*, 33(**1**), 25–34.

Khanna, P., Ong, C., Bay, B.H., Baeg, G.H. (2015). Nanotoxicity: an interplay of oxidative stress, inflammation and cell death. *Nanomaterials,* 5(**3**), 1163–1180.

Kim, H. S. (2005). Do not put too much value on conventional medicines. *J. Ethnopharmacol*., 100, 37–39.

Kim, S. Y., Kim, E. A., Kim, Y. S., Yu, S. K., Choi, C., Lee, J. S., Kim, Y. T., Nah, J. W., and Jeon, Y. J. (2016). Protective effects of polysaccharides from *Psidium guajava* leave against oxidative stresses. *International Journal of Biol. Macromol.* , 91, 804–811.

Komazin, G., Maybin, M., Woodard, R. W., Scior, T., Schwudke, D., Schombel, U., Gisch, N., Mamat, U., and Meredith, T. C. (2019). Substrate structure-activity relationship reveals a limited lipopolysaccharide chemotype range for intestinal alkaline phosphatase. The *Journal of Biological Chemistry*, 294(**50**), 19405-19423.

Korani, M., Rezayat, S. M., Gilani, K., Arbabi-Bidgoli, S., and Adeli, S. (2011). Acute and subchronic dermal toxicity of nanosilver in guinea pig. *International Journal of Nanomedicine*, 1(**6**), 855-862.

Krishna, M. (2013). Microscopic Anatomy of the Liver. Clinical Liver Disease, 2 (Suppl 1), S4.

Kumar, M., Dahuja, A., Sachdev, A., Kaur, C., Varghese, E., Saha, S. and Sairam, K. V. S. S. (2019). Valorisation of black carrot pomace: Microwave assisted extraction of bioactive phytoceuticals and antioxidant activity using Box–Behnken design. *J. Food Sci. Technol*., 56, 995–1007.

Kun, J., Sameer, A., and Barbara, A. C. (2018). Primary liver cancers-part 1: Histopathology, differential diagnoses, and risk stratification. Cancer control, 25, 1-26.

Laily, N., Kusumaningtyas, R. W., Sukarti, I., Rini, M.R.D.K. (2015). The potency of guava *Psidium guajava* (L.) leaves as a functional immunostimulatory ingredient. *Procedia Chem*istry, 14, 301-307.

Lautt, W. W. (2009). Hepatic circulation: Physiology and pathophysiology. San Rafael (CA): Morgan and claypool life sciences. Chapter 2, overview.

Leung, K. K., and Hirschfield, G. M. (2022). Elevated serum aminotransferases. *The Journal of the American Medical Association*, 327(**6**), 580-581.

Liu, Y., Jin, X., and Chen, Z. (2018). The formation of iron nanoparticles by Eucalyptus leaf extract and used to remove Cr (VI). *Science of the Total Environment*, 627, 470–479.

Löhr, J. M., Panic, N., Vujasinovic, M., and Verbeke, C. S. (2018). The Ageing Pancreas: A Systematic Review of the Evidence and Analysis of the Consequences. Journal of Internal Medicine, 283(**5**), 446-460.

Long, M. T., and Friedman, L. S. (2014). Hepatic Structure and Function. Gastrointestinal Anatomy and Physiology: The Essentials, 129-148.

Lopez-Rubio, A., Fabra, M.J., Martínez-Sanz, M. (2019). Food packaging based on nanomaterials. *Journal of Biological Chemistry,* 2(**5**), 23- 25.

Lowry, O. H., Rosebrough, N. J., Farr, A. L., and Randall, R. J. (1951). Protein measurement with the Folin phenol reagent. *Journal of Biological Chemistry,* 193(**1**), 265-275**.**

Lung, T., Sakem, B., Risch, L., Würzner, R., Colucci, G., Cerny, A., and Nydegger, U. (2019). The complement system in liver diseases: Evidence-based approach and therapeutic options. *Journal of Translational Autoimmunity*, 2, 100017.

Ma, Y., Yang, M., He, Z., Wei, Q., and Li, J. (2017). The biological function of kupffer cells in liver disease. In (Ed.), Biology of Myelomonocytic Cells. IntechOpen, 54-84.

Macpherson, I., Nobes, J. H., Dow, E., Furrie, E., Miller, M. H., Robinson, E. M., and Dillon, J. F. (2020). Intelligent liver function testing: Working smarter to improve patient outcomes in diver disease. *The Journal of Applied Laboratory Medicine*, 5(**5**), 1090 1100.

Malakouti, M., Kataria, A., Ali, S. K., and Schenker, S. (2017). Elevated Liver Enzymes in Asymptomatic Patients – What Should I Do? *Journal of Clinical and Translational Hepatology*, 5(**4**), 394-403.

Malik, D. S., Jain, C. K., and Yadav, A. K. (2015). Preparation and characterization of plant based low cost adsorbents. *Journal of Global Biosciences*, 4(**1**), 1824–1831.

Manoj, A., and Annamma, P. (2019). An Architecture of microscopic anatomy of human liver. *World Journal of Pharmaceutical and Medical Research*, 5(**5**), 101-105.

Maruyama, H., and Shiina, S. (2020). Antioxidant Therapy on ischemic hepatitis: Here we are and where do we go. *Hepatology International*, 14, 456–459.

Maslak, E., Gregorius, A., and Chlopicki, S. (2015). liver sinusoidal endothelial cells (LSECs) function and NAFLD; NO-based Therapy targeted to the liver. *Pharmacological Reports*, 67, 689-694.

Matsuda, K., Nishimura, Y., Kurata, N., Iwase, M. and Yasuhara, H. (2007). Effects of continuous ingestion of herbal teas on intestinal CYP3A in the rat. *Journal of Pharmacological Science,* 103*,* 214–221.

Matthew H. M. D. (2014). The 3D structure of the liver (www.webmd.com)

Matyas, C., Haskó, G., Liaudet, L., Trojnar, E., and Pacher, P. (2021). Interplay of cardiovascular mediators, oxidative stress and inflammation in liver disease and its complications. *Nature Reviews Cardiology*, 18(**2**), 117-135.

McClements, D.J., Xiao, H. (2012). Potential biological fate of ingested nanoemulsions: influence of particle characteristics. *Food Function.* 3(**3**), 202–220.

McCord, J. M., and Fridovich, I. (1969). Superoxide dismutase: An enzymic function for erythrocuprein (hemocuprein). *Journal of Biological Chemistry*, 244(**22**), 6049–6055.

Modusolumuo, M. A. (2011). Man's exposure to chemicals substance and its sundry Consequences. 11th inaugural lecture, Federal University of Technology Yola, Adamawa State, Nigeria.

Mohammadian, M., Waly, M.I., Moghadam, M., Emam-Djomeh, Z., Salami, M., Moosavi Movahedi, A.A. (2020). Nanostructured food proteins as efficient systems for the encapsulation of bioactive compounds. *Food Sci. Hum. Wellness*, 9(**3**), 199–213.

Mohd, A. H., Marghoob, H., and Abdelmarouf, M. (2016). Comparative Study of 5' Nucleotidase Test in Various Liver Diseases. *Journal of Clinical and Diagnostic Research*, 10(**2**), 1-3.

Moraru, C., Huang, Q., Takhistov, P., Dogan, H., Kokini, J. (2009). Food nanotechnology: current developments and future prospects. In: Global Issues in Food Science and Technology. *Elsevier*, 369–399.

Mueller, S. (2020). Liver elastography clinical use and interpretation Cham: Springer), 19, 737.

Mühlfeld, C., Gerh, P., and Rothen-Rutishauser, B. (2008). Translocation and cellular entering mechanisms of nanoparticles in the respiratory trait. *Swiss Medical Weekly Review*, 138, 387 – 391.

Nair, S. S., Kavrekar, V. and Mishra, A. (2013). In vitro studies on alpha amylase and alpha glucosidase inhibitory activities of selected plant extracts. *European Journal of Experimental Biol*ogy, 3, 128–132.

Newman, D.J., Cragg, G. M., and Snader, K. M. (2003). Natural products as sources of new drugs over the period 1981–2002. *Journal Nat. Prod.*, 66, 1022–1037.

Nile, S.H., Kai, G., 2021. Recent clinical trials on natural products and traditional Chinese medicine combating the COVID-19. *Indian Journal of Microbiology*, 61(**1**), 10–15.

Nishikimi, M., Rao, N. A., and Yagi, K. (1972). The occurrence of superoxide anion in the reaction of reduced phenazine methosulfate and molecular oxygen. *Biochemical and Biophysical Research Communications*, 46(**2**), 849–854.

Njoku, D. B. (2014). Drug-induced hepatotoxicity: metabolic, genetic and immunological basis. *International Journal of Molecular Science,* 15(**4**), 6990-7003.

Ogunyemi, S. O. (2019). Green synthesis of zinc oxide nanoparticles using different plant extracts and their antibacterial properties. *Arabian Journal of Chemistry,* 12(**8**), 2234–2251.

Ojewole, J. A. O., Awe, E. O. and Chiwororo, W. D. H. (2008). Antidiarrhoeal activity of *Psidium guajava* Linn. (Myrtaceae) leaf aqueous extract in rodents. *Journal of Smooth Muscle Research*, 44, 195–207.

Ojha, S., Kumar, B. (2018). A review on nanotechnology based innovations in diagnosis and treatment of multiple sclerosis. Journal of Cellular Immun. 4(**2**), 56–64.

Omerovic, N., Djisalov, M., Zivojevic, K., Mladenovic, M., Vunduk, J., Milenkovic, I., Knezevic, N.Z., Gadjanski, I., Vidic, J. (2021). Antimicrobial nanoparticles and biodegradable polymer composites for active food packaging applications. *Compr. Rev. Food Sci. Food Saf.* 20 (**3**), 2428–2454.

Ono, S., Egawa, G., and Kabashima, K. (2017). Regulation of Blood Vascular Permeability in the Skin. Inflammation and Regeneration, 37, 11.

Ozimek, L., Pospiech, E., Narine, S., 2010. Nanotechnologies in food and meat processing. ACTA Scientiarum Polonorum Technologia Alimentaria 9 (4), 401–412.

Pan, Z., Lin, Y., Sarkar, B., Owens, G., and Chen, Z. (2020). Green synthesis of iron nanoparticles using red peanut skin extract: Synthesis mechanism, characterization and effect of conditions on chromium removal. *Journal of Colloid and Interface Science*, 55(**8**), 106-114.

Pathakoti, K., Manubolu, M., Hwang, H.-M. (2017). Nanostructures: current uses and future applications in food science. *Journal. Food Drug Anal.* 25(**2**), 245–253.

Patra, J.K., Shin, H.-S., Paramithiotis, S. (2018). Application of nanotechnology in food science and food microbiology. *Frontier Microbiology*, 9, 714.

Perkins, E. J., Bao, W. and Guan, X. (2006). Comparison of transcriptional responses in liver tissue and primary hepatocyte cell cultures after exposure to hexahydro-1, 3, 5-trinitro-1, 3, 5-triazine. *BMC Bioinformatics*, 7(**2**), 2.

Pietro, M., Gilles, M., Christian, T., Philippe, M., Heinz, O., and Peitgen, J. H. D. (2014). Anatomy of the liver: An outline with three levels of complexity – A further step towards tailored territorial liver resections. *Journal of Hepatology*, 60(**3**), 654-662.

Poisson, J., Lemoinne, S., Boulanger, C., Durand, F., Moreau, R., Valla, D., and Rautou, P. E. (2017). Liver Sinusoidal Endothelial Cells: Physiology and Role in Liver Diseases. *Journal of Hepathology*, 66(**1**), 212-227.

Punia, S. and Kumar, M. (2021). Litchi (*Litchi chinenis*) seed: Nutritional profile, bioactivities, and its industrial applications. *Trends Food Science and Technology*, 108, 58–70.

Punia, S., Sandhu, K. S., Grasso, S., Purewal, S. S., Kaur, M., Siroha, A. K., Kumar, K., Kumar, V. and Kumar, M. (2020). *Aspergillus oryzae* fermented rice bran: A byproduct with enhanced bioactive compounds and antioxidant potential. *Foods*, 10, 70.

Rahul, B., Mahabub, A., Animesh, S., Ismail,H. M.D, Moinul, H. and Mominul, H. (2022). Application of nanotechnology in food: processing, preservation, packaging and safety assessment. *Heliyon*, 8(2022) e11795.

Rajesh, M. (2021). Environmental risk factors implicated in liver disease: A mini-review. *Frontiers in Public Health*, 9, 683719.

Ramesh, C. S., and Sharma, M. (2014). Biliary Tract Anatomy and Its Relationship with Venous Drainage. Journal of Clinical and Experimental Hepatology, 4(1), 18-26.

Reitman, S. and Frankel, S. (1957). Method of alanine and aspartate aminotransferase determination. *American Journal of Clinical Patholology*, 28, 56–58.

Reuben, A. (2016). Examination of the abdomen. *Clinical Liver Disease*, 7(**6**), 143-150.

Ryan, M. G., and Neil, D. (2021). Rappaport, glisson, hering, and mall-champions of liver microanatomy: Microscopic and ultramicroscopic anatomy of the liver into the modern Age. *Clinical Liver Diseases,* 18, 76-92.

Saar, I., and Brysch, W. (2020). U.S. Patent Application No. 16/977,655.

Sabatino, A., Regolisti, G., Karupaiah, T., Sahathevan, S., Singh, B. K. S., Khor, B. H., Salhab, N., Karavetian, M., Cupisti, A., and Fiaccadori, E. (2017). Protein-energy wasting and nutritional supplementation in patients with end-stage renal disease on hemodialysis. *Clinical Nutrition*, 36, 663–671.

Sachan, R., and Singh, R. (2018). Chemical induced liver injury: Types, mechanisms and biomarkers. *EndPress Anatomical Science*, 6(1)

Sahoo, M., Vishwakarma, S., Panigrahi, C., and Kumar, J. (2021). Nanotechnology: current applications and future scope in food. *Food Frontiers*, 2(**1**), 3–22.

Saini, R. (2013). Nanotechnology: The future medicine. *Journals of Cutaneous and Aesthetic Surgery,* 3(**1**), 32–33.

Salau, A. K., Yakubu, M. T., and Oladiji, A. T. (2013). Cytotoxic activity of aqueous extracts of anogeissus leiocarpus and terminalia avicennioides root barks against ehrlich ascites carcinoma cells. *Indian Journal of Pharmacology*, 45(**4**), 381.

Sanz-García, C., Fernández-Iglesias, A., Gracia-Sancho, J., Arráez-Aybar, L. A., Nevzorova, Y. A., and Cubero, F. J. (2021). The space of disse: The liver hub in health and disease. *Livers*, 1(**1**), 3-26.

Saranyaadevi, K. V., Subha, V., Ernest, R., and Renganathan, S. (2014). Synthesis and characterization of copper nanoparticle using *Capparis zeylanica* leaf extract. *International Journal of Chemical Technology Research*, 6(**10**), 4533–4541.

Satoshi, K., Kazuto, K., Toshifumi, G., Osamu, M., Wataru, K., Miho, O., Kenichiro, O., Takumi, S., and Takahiro, O. (2020). Pathophysiology and Imaging Findings of Bile Duct Necrosis: A Rare but Serious Complication of Transarterial Therapy for Liver Tumors. *Cancers*, 12, 2596

Schleh, C., Semmler-Behnke, M., Lipka, J., Wenk, A., Hirn, S., Schäffler, M., Schmid, G., Simon, U., Kreyling, W. G. (2012). Size and surface charge of gold nanoparticles determine absorption across intestinal barriers and accumulation in secondary target organs after oral administration. *Nano-toxicology*, 6, 36-46.

Shabbir, H., Kausar, T., Noreen, S., Hussain, A., Huang, Q., Gani, A., Su, S., and Nawaz, A. (2020). In vivo screening and antidiabetic potential of polyphenol extracts from guava pulp, seeds and leaves. *Animals*, 10, 1714.

Shao, M., Wang, Y. Liu, Z., Zhang, D. M., Cao, H. H., Jiang, R. W., Fan, C. L., Zhang, X. Q., Chen, H. R., Yao, X.S. (2010). Psiguadials A and B, two novel meroterpenoids with unusual skeletons from the leaves of *Psidium guajava*. *Org. Lett.* , 12, 5040–5043.

Sharma, M., Somani, P., Rameshbabu, C. S., Sunkara, T., and Rai, P. (2018). Stepwise Evaluation of liver sectors and liver segments by endoscopic ultrasound. *World Journal of Gastrointestinal Enterology*, 10(**11**), 326-339.

Sharma, R., Jafari, S.M., Sharma, S., 2020. Antimicrobial bio-nanocomposites and their potential applications in food packaging. *Food Control*, 112, 107086.

Siddiqi, K.S., Husen, A., Rao, R.A., 2018. A review on biosynthesis of silver nanoparticles and their biocidal properties. J. Nanobiotechnol. 16(**1**), 1–28.

Singh, A., Chandrashekhara, S. H., Handa, N., Baliyan, V., and Kumar, P. (2016). Periportal Neoplasms-a CT Perspective: Review Article. *The British journal of Radiology,* 89(**1060**), 20150756.

Singh, R. P., Ramarao, P., and Kakkar, P. (2019). Hepatotoxicity of engineered nanoparticles: Understanding mechanisms and future perspectives. *Archives of Toxicology*, 93(**8**), 2457–2486.

Sivakami, M., Devi, K. R., and Renuka, R. (2021). Green synthesis of magnetic nanoparticles by *Murraya koenigii* leaves extract for biomedical application. *Materials Today: Proceedings*, 36, 567-573.

Skandalakis, J. E., Skandalakis, L. J., Skandalakis, P. N., and Mirilas, P. (2004). Hepatic Surgical Anatomy. *Surgical Clinics*, 84(**2**), 413-435.

Smith, R.M.; Oliveros-Belardo, L. The composition of leaf essential oils of *Psidium guajava L.* from Manila, Philippines. *Asian Journal Pharm.*, 1(**3**), 5–9.

Solass, W., Struller, F., Horvath, P., Konigrainer, A., Sipos, B., and Weinreich, F. J. (2016). Morphology of the peritoneal cavity and pathophysiological conseqauences. *Pleura and Peritoneum,* 1(**4**), 193-201.

Sowemimo, A., Okwuchuku, E., Samuel, F. M., Ayoola, O., and Mutiat, I. (2015). Musanga cecropioides leaf extract exhibits anti-inflammatory and anti-nociceptive activities in animal models. *Revista Brasileira de Farmacognosia*, 25, 506-512.

Spinazzi, M., Angelini, C., and Patrini, C. (2010). Subacute sensory ataxia and optic neuropathy with thiamine deficiency. *Nature Reviews Neurology*, 6(**5**), 288-293.

Srinivasan, K., Sivasubramanian, S., and Kumaravel, S. (2013). Phytochemical profiling and GC-MS study of *Adhatoda vasica* leaves. *International Journal of Pharmaceutical and Bio Sciences*, 5(**1**), 714-720.

Stefanis, L., Burke, R. E. and Greene, L. A. (1997). Apoptosis in neurodegenerative disorders. *Curr. Opin. Neurol.*, 10, 299–305.

Szafranska, K., Kruse, L. D., Holte, C. F., McCourt, P., and Zapotoczny, B. (2021). The whole story about fenestrations in LSEC. *Frontiers in physiology*, 12, 735573.

Tanaka, M., and Iwakiri, Y. (2018). Lymphatics in the liver. *Current opinion in immunology*, 53, 137-142.

Tanimizu, N., Ichinohe, N., Sasaki, Y., Itoh, T., Sudo, R., Yamaguchi, T., Katsuda, T., Ninomiya, T., Tokino, T., Ochiya, T., Miyajima, A., and Mitaka, T. (2021). Generation of functional liver organoids on combining hepatocytes and cholangiocytes with hepatobiliary connections ex vivo. *Nature Communications*, 12, 3390.

Terasaki, F., Yamamoto, Y., Sugiura, T., Okamura, Y., Ito, T., Ashida, R., Ohgi, K., Aramaki, T., and Uesaka, K. (2021). Analysis of right-sided ligamentum teres: The novel anatomical findings and classification. *Journal of Hepato-Biliary-Pancreatic Sciences*, 28(**2**), 221-230.

Tian, C. R., Qian, L., Shen, X. Z., Li, J. J., and Wen, J. T. (2014). Distribution of Serum Total Protein in Elderly Chinese. PLoS ONE, 9, 101242.

Tietz, N.W. (1995). Clinical Guide to laboratory Tests 3rd edition. W.B. Sanders company, Philadephia U.S.A.555-556

Torres Rojas, A. M., Lorente, S., Hautefeuille, M., and Sanchez-Cedillo, A. (2021). Hierarchical Modeling of the Liver Vascular System. *Frontiers in Physiology*, 12(**73**), 31- 65.

Toyokuni, S. (2016). Oxidative stress as an iceberg in carcinogenesis and cancer biology. *Arch. Biochem. Biophys.*, 595, 46–49.

Ullah, F., Ayaz, M., Sadiq, A., Ullah, F., Hussain, I., Shahid, M., Yessimbekov, Z., Adhikari-Devkota, A. and Devkota, H. P. (2020). Potential role of plant extracts and phytochemicals against foodborne pathogens. *Appl. Sci.*, 10, 4597.

Verma, D., Gulati, N., Kaul, S., Mukherjee, S., Nagaich, U., 2018. Protein based nanostructures for drug delivery. J. Pharm.

Villa-Suárez, J. M., García-Fontana, C., Andújar-Vera, F., González-Salvatierra, S., de Haro Muñoz, T., Contreras-Bolívar, V., García-Fontana, B., and Muñoz-Torres, M. (2021). Hypophosphatasia: A Unique Disorder of Bone Mineralization. International Journal of Molecular Sciences. 22(9), 4303.

Wallace, K., Burt, A. D., and Wright, M. C. (2008). Liver Fibrosis. *Biochemical Journal*, 411(**1**), 1-18.

Wang, J. W., Yu, C. H., Hou, W. C., Hsiao, T. C., and Lin, Y. P. (2024). Characterization of Fe-containing and Pb-containing nanoparticles resulting from corrosion of plumbing materials in tap water using a hyphenated ATM-DMA-spICP-MS system. *Environmental Science and Technology*, 58(**4**), 2038-2047.

Wang, M., Li, S., Chen, Z., Zhu, J., Hao, W., Jia, G., Chen, W., Zheng, Y., Qu, W., Liu, Y., 2021. Safety assessment of nanoparticles in food: current status and prospective. *Nano Today* 39, 101169.

Woldeyes, D. H. (2019). The Occurrence of an Additional (Accessory) Lobe of Liver and Undescended Testis in a Single Cadaver: A Case Report. Journal of Medical Case Reports, 13, 1-5.

Wu, T., Tang, M., and He, Q. (2014). Review of the effects of manufactured nanoparticles on mammalian target organs. *Nanotoxicology*, 8(**1**), 107-116.

Wyser, Y., Adams, M., Avella, M., Carlander, D., Garcia, L., Pieper, G., Rennen, M., Schuermans, J., Weiss, J., (2016). Outlook and challenges of nanotechnologies for food packaging. *Package technology sciences,* 29(**12**), 615–648.

Xu, Q., Kambhampati, S.P., Kannan, R.M., 2013. Nanotechnology approaches for ocular drug delivery. *Middle East African Journal*, 20(**1**), 26.

Yakubu, O. E., Ojogbane, E., Abu, M. S., Shaibu, C. O., and Ayegba W. E. (2020). Haematinic Effects of Ethanol Extract of Ficus sur Leaves on Diethylnitrosamine-induced Toxicity in Wistar Rats. *Journal of pharmacology and Toxicology*, 15, 16-21.

Yao, X., He, C., Chen, Y., and Zhao, W. (2020). The toxicity of metallic nanoparticles on liver: the subcellular damages, mechanisms, and outcomes, *International Journal of Nanomedicine,* 15, 3947-3960.

Zhang, Z., Kong, F., Ni, H., Mo, Z., Wan, J. B., Hua, D., and Yan, C. (2016). Structural characterization, α-glucosidase inhibitory and DPPH scavenging activities of polysaccharides from guava. *Carbohydrate. Polym.* , 144, 106–114.

Zimet, P., Livney, Y.D., 2009. Beta-lactoglobulin and its nanocomplexes with pectin as vehicles for ω-3 polyunsaturated fatty acids. Food Hydrocolloids 23(**4**), 1120–1126.